Testing the hypothesis of a link between Earth's magnetic field and climate change: a case study from southern Sweden focusing on the 1st millennium BC

Wenxin Ning

Dissertations in Geology at Lund University,
Master's thesis, no 290
(45 hp/ECTS credits)

Department of Earth and Ecosystem Sciences
Division of Geology
Lund University
2011

Testing the hypothesis of a link between Earth's magnetic field and climate change: a case study from southern Sweden focusing on the 1st millennium BC

Master Thesis

Wenxin Ning

Department of Earth and Ecosystem Sciences

Lund University

2011

Contents

Cover Picture: Working on the ice cover of Lake Gyltigesjön, southern Sweden

Testing the hypothesis of a link between Earth's magnetic field and climate change: a case study from southern Sweden focusing on the 1st millennium BC

WENXIN NING

Ning, W., 2011: Testing the hypothesis of a link between Earth's magnetic field and climate change: a case study from southern Sweden focusing on the 1st millennium BC. *Examensarbeten i geologi vid Lunds universitet*, No. 290, 35pp. 45 ECTS credits.

Abstract: It is commonly believed that long-term (10 to 1000 kyr) and short-term (10 to 1000 years) climatic changes on Earth can be interpreted by periodic variations in Earth's orbit around the Sun and variations in solar irradiance, respectively. In recent years, geomagnetic field changes have been suggested as a potential driver of climate change. However, a link between these two factors is not straightforward. A relationship between geomagnetic field changes and climate is still debatable. To test the hypothesis of a link between past changes in the geomagnetic field and climate, reliable reconstructions of paleoclimate and paleogeomagnetic field are needed. In this study, high resolution paleomagnetic and paleoecological records obtained from varved sediments in Lake Gyltigesjön, southern Sweden, with an emphasis on the 1st millennium BC, are directly compared to test the hypothesis. The 1st millennium BC is one of the most interesting periods of geomagnetic variation during the Holocene, which is characterized in paleomagnetic records by high magnetic field intensity and relatively abrupt geomagnetic pole movement. Through measurements of magnetic hysteresis parameters and First Order Reversal Curves (FORCs), sediments from Gyltigesjön are believed to contain abundant single domain (SD) magnetite grains, which are an excellent source of paleomagnetic field reconstructions. In order to reconstruct paleoclimate conditions during the 1st millennium BC, pollen analysis, measurements of varve thickness, loss on ignition (LOI), total organic carbon (TC), ration of C/N, grey scale and magnetic parameters were conducted. The main conclusion is that no evidence of a link between geomagnetic field and climate change can be found in southern Sweden during the study period. Early human activity, however, could have masked the palaeoclimatic significance of the proxies used.

Keywords: Paleomagnetism, varve, lake sediment, southern Sweden, climate reconstruction, human impact.

Wenxin Ning, Department of Earth and Ecosystem Sciences, Lund University, Sölvegatan 12, SE-223 62 Lund, Sweden. E-mail: ningwenxin@telia.com

Testing the hypothesis of a link between Earth's magnetic field and climate change: a case study from southern Sweden focusing on the 1st millennium BC

WENXIN NING

Ning, W., 2011: Testing the hypothesis of a link between Earth's magnetic field and climate change: a case study from southern Sweden focusing on the 1st millennium BC. *Examensarbeten i geologi vid Lunds universitet*, Nr. 290, 35s. 45 hp.

Under senare år har förändringar i det jordmagnetiska fältet föreslagits som en möjlig drivkraft för klimatförändringar. Det finns dock inget enkelt samband mellan dessa två faktorer. Ett samband mellan förändringar i det jordmagnetiska fältet och klimatet är fortfarande omdebatterat. För att testa hypotesen om ett samband mellan tidigare förändringar i det jordmagnetiska fältet och klimatet behövs tillförlitliga rekonstruktioner av det gångna klimatet och jordmagnetiska fältet. I denna studie har högupplösta paleomagnetiska och paleoekologiska arkiv från varviga sediment i Gyltigesjön i södra Sverige direkt jämförts för att testa hypotesen, med betoning på det första årtusendet f.Kr. Det första årtusendet f.Kr. är en av de mest intressanta perioderna för jordmagnetiska variationer under Holocen, vilket i paleomagnetiska arkiv kännetecknas av en hög jordmagnetisk intensitet och en relativt abrupt jordmagnetisk polrörelse. Genom mätningar av parametrar för magnetisk hysteres och "First Order Reversal Curves" (FORCs) antas sedimenten i Gyltigesjön innehålla rikligt med magnetitkorn av enda domän (SD) vilket är en utmärkt källa vid rekonstruktioner av det jordmagnetiska fältet. För att rekonstruera de paleoklimatiska förhållandena under det första årtusendet f.Kr. utfördes: pollenanalys, mätningar av varvtjocklek, glödförlust (LOI), totalt kol (TC), förhållande mellan kol och kväve (C/N), gråskala och mätningar av magnetiska parametrar. Den huvudsakliga slutsatsen är att det inte hittats något bevis för ett samband mellan jordens magnetfält och klimatförändringar i södra Sverige under den studerade perioden. Tidig mänsklig aktivitet kan dock ha påverkat betydelsen av de klimatproxies som har använts.

Keywords: Paleomagnetism, varve, sjösediment, södra Sverige, klimat återuppbyggnad, mänsklig påverkan.

Wenxin Ning, Geologiska Instirutionen, Centrum för GeoBiosfärsvetenskap, Lunds Universitet, Sölvegatan 12, 22362 Lund,Sverige. E-post:ningwenxin@gmail.com

1 Introduction

1.1 Varved sediments in Sweden

Varved (annually laminated) lake sediments in Sweden have frequently been used for dating and reconstructing past environmental changes. The word *varve* was first formally used by the Swedish scientist Gerard De Geer at the eleventh International Geological Congress in Stockholm in 1910 (Stanton 2011). He claimed that distinct laminations in Swedish glacial lake sediments were annual in nature and could be used as the basis of a Swedish timescales back to the last deglaciation (Stanton 2011). For a long time, studies focused on these clastic varves rather than the more organic rich biogenic/clastic varves found in relatively small post-glacial lakes. It was not until the 1970's that investigations of biogenic/clastic varves became more extensive ((Renberg 1982); Petterson, 1996; Zillén et al., 2003). These studies have focused on paleoclimate (Snowball et al. 2002), mineral magnetism (Snowball et al. 1999) and paleomagnetism (Snowball & Sandgren 2004; Snowball et al. 2007).

Understanding the formation process of the biogenic/clastic varves is essential for their application. According to Renberg (1982), one common varve contains a threefold structure. The lowest part of a varve is composed of light-colored mineral matter. This light layer most likely originates from stream bank erosion during periods of maximum spring discharge (Snowball et al. 1999). Gradually this lamina grades upwards into a dark layer which is mainly composed of organic particulate material. The source of the organic material can be plant fibres, algae, pollen and so on. Minor amounts of fine-grained mineral matter also exist in this layer. These two laminaes are generated before the lake is covered with ice. A varve is completed by a darker thin lamina on top, which is composed of fine-grained organic material deposited in calm water when the lake is covered by ice. Such varve formation is commonly found in small lakes in Fennoscanadia (Zillén et al. 2003). In this thesis, such biogenic/clastic varves from a Swedish lake in the province of Halland are studied.

1.2 Reconstruction of paleomagnetic field with varved sediments

Reconstructions of the geomagnetic field have profound significance. Applications include the investigation of prehistorical solar activity (Snowball & Muscheler 2007), reconstructions of geomagnetic field variations and modeling (Nilsson 2011) and the use of these for relative dating (Snowball et al. 2007). All of these applications need a precise reconstruction of the paleomagnetic field. Changes of the geomagnetic field through time are collectively termed palaeomagnetic secular variation (PSV). PSV records are composed of intensity (strength of the geomagnetic field), declination (angle between the magnetic north and geographic north) and inclination (angle between the vertical magnetic field lines and the horizontal plane). For the contemporary geomagnetic field, the inclination is steepest at the magnetic poles (90°) and shallowest at the magnetic equator (0°). The geomagnetic field intensity at Earth's surface is highest at the poles (maximum ca. 60 μT) and lowest at the equator (maximum ca. 30 μT) (Stanton 2010).

Geomagnetic field reconstructions beyond the limits of historical observations (c. 400 years) rely primarily on natural remanent magnetizations (NRMs) stored in geological materials or archeological archives. Both extrusive rocks and baked archaeological artefacts are able to acquire thermoremanent magnetism (TRM), through which paleointensity can be reconstructed (Stanton 2011). Unfortunately, it is difficult to find these

materials continuously both in space and time (Haltia-Hovi et al. 2011). Magnetic minerals (e.g. magnetite and hematite) can align to the geomagnetic field closely after the time of deposition and, therefore, sediments formed in lakes and marines can record changes in the geomagnetic field. This mechanism is called detrital remnant magnetism (DRM). Compared to marine sediments, continental lake sediments are relatively easier to recover intact and achieve more precise chronology (Snowball et al. 2007). Reconstructions of geomagnetic field variations for the Holocene epoch are dominated by studies of continental lakes. Swedish varved lake sediments have been proved to be excellent material for palaeomagnetic studies (Snowball & Sandgren, 2004; Snowball et al. 2007). Based on data collected from six varved lakes in Sweden and Finland, Ian Snowball et al. (2007) have reconstructed a palaeomagnetic secular variation master curve (FENNOSTACK) and relative palaeointensity curve (FENNORPIS) for Fennoscandia that cover the last 10,000 years.

1.3 Advantage of varved sediments in paleoclimate study and dating

Varved sediment is also an ideal natural archive for palaeoclimate studies (Haltia-Hovi et al. 2011; Snowball et al. 2002). It is possible to precisely reconstruct the sediment accumulation rate during a determined period of time. For example, pollen influx can be calculated quite accurately with varved sediments compared to non-varved sediments. The thickness of varves can be linked to precipitation, water discharge, temperature and land use changes (Gälman et al. 2005; Wohlfarth et al. 1997). Together with TC, C/N, diatom analysis and so on, varved sediments can, theoretically, provide abundant information about paleoclimate at an annual, or even seasonal, resolution. More importantly, with the feature of annual lamination, a precise chronology can be obtained through counting the varves (Snowball et al. 1999). It is sometimes necessary to secure a floating varve chronology to a calendar year timescale using additional dating methods (Stanton et al. 2010). Varved sediment is also good material for the radiocarbon 'wiggle match' dating method, through which a more precise dating result can be expected (Snowball et al. 2010).

1.4 Connection between paleomagnetism and climate?

It is commonly believed that long-term climatic changes (10 to 1000 kyr) on Earth are governed by periodic variations in Earth's orbit around the Sun, leading to alternating glacial and interglacial. Climatic variations that take place over shorter timescales (10 to 1000 years) cannot be related to orbital (Milankovic) forcing. For example, the Little Ice Age (~AD 1550 to 1850) and the transition to a colder period at ca. 2800 cal. BP, are thought to have been driven by variations in solar irradiance (Geel et al. 2000; Geel et al. 1996).

As more high quality paleomagnetic data have been derived, recent studies hypothesize that geomagnetic changes can also cause centennial climate change (Gallet et al. 2005; Courtillot et al. 2007; Knudsen & Riisager, 2009). Gallet et al. (2005) found that rapid intensity increases during the last few thousand years coincided with the occurrence of cooling periods. They suggest that enhanced secular variation of the geomagnetic field may have had a significant influence on the climatic variations observed in Western Europe during the past few millennia. Knudsen & Riisager (2009) claim there is a positive correlation between geomagnetic dipole moment and speleothem $\delta^{18}O$ records from Oman and southern China. They conclude there is a link between Earth's magnetic field and low-latitude precipitation over the most recent 5000 years.

One problem with these studies is that the geomagnetic records and climate proxy data are not acquired from the same site. Errors in the

different chronologies make it difficult to compare the records at centennial scales (Bard & Delaygue 2007). Data for paleogeomagnetic reconstructions are limited in the studies by Gallet et al. (2005) and Courtillot et al. (2007), making the hypothesis of a link between the geomagnetic field and climate difficult to assess. The relationship between geomagnetism and climate has not been fully understood. Those who believe that there is connection between geomagnetism and climate speculate on the relationship (Courtillot et al. 2007; Knudsen & Riisager 2009). One of most popular theories is the Galactic cosmic ray (GCR)-climate theory (Carslaw et al. 2002). However, this theory is not able to explain all the relationships observed (Courtillot et al. 2007). The relationship between geomagnetic field and climate remains debatable.

1.5 Aim of this study

In this study, high resolution PSV and palaeointensity data and proxy indicators of environmental change derived from the same sediment sequence are directly compared, focusing on one period with distinct geomagnetic field variability around 2600 cal. yrs BP. The timing of a distinct geomagnetic field change during the 1st Millennium BC in northern Europe, which is characterized by a distinct westerly swing in declination (the easterly starting point known as feature "f") is interesting. This millennium was chosen for this study because this is one of the most interesting periods concerning geomagnetic variation in the Holocene epoch. In this study, the reliability of the palaeomagnetic reconstruction will be tested. Furthermore, the high resolution paleoclimate and paleogeomagnetic reconstructions outlined here form a test of the geomagnetism-climate hypothesis in southern Sweden.

There is evidence that human activity already existing in southern Sweden within the 1st Millennium BC (Jong 2006). Human activity going on in or near the lake's catchment during the study period could affect the local proxy environmental data and create a bias in the relative palaeointensity data (Stanton 2011). This human activity could possibly also mask the significance of climate signal. On the other hand, the shift to wetter and colder conditions caused by solar forcing around 2800 cal. yrs BP is thought to have worldwide significance (Geel et al. 1996, 1998) and one would expect such a signal to be present in palaeoclimatic data sets.

2 Site description

2.1 Location, morphology of Gyltigesjön and regional vegetation

Lake Gyltigesjön (56°45'21"N, 13°10'34"E) is located in the province of Halland, southwest Sweden (*Figure. 1*). The lake lies 65.7 m a.s.l and it covers ~0.4 km^2 with a quite elongated shape. It has a mean water depth of 9.1 m and the maximum depth is 20 m. Water volume of Gyltigesjön is 3.6 million m^3 and the average turnover time is as short as about 10 days. The catchment area is 172 km^2 and the main habitat in the catchment is forest, which currently represents 61% of the surface (~104 km^2). The forest mainly consists of birch, pine, alder and oak, and was observed during one excursion to Gyltigesjön in early 2011. A quarter of the catchment surface consists of marsh (~44 km^2) and a small portion (8%) consists of open land. The remaining 6% of the surface is water, including Lake Gyltigesjön itself. The above information of Gyltigesjön is taken from webpage of Department of Environmental Assessment, Uppsala (http://info1.ma.slu.se/IKEU/Gyltigesjon/pg1.html).

Lake Gyltigesjön is relatively deep compared to its surface area and this character makes it easier for stratification to occur, which can lead to anaerobic bottom water conditions. The absence of oxygen condition forms a barrier

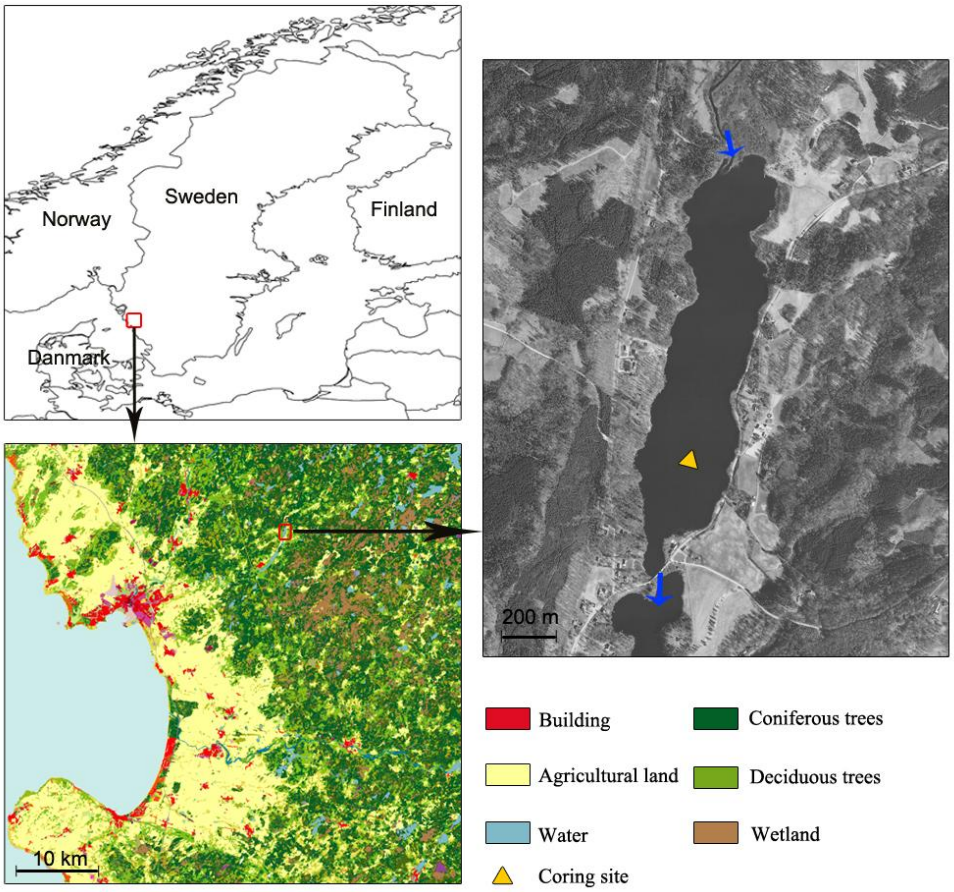

Fig. 1. *Map showing the location of Gyltigesjön and the coring site (yellow filled triangle). Locations of main inlet and outlet are shown as blue arrow.*

to bottom dwelling fauna and prevents bioturbation by macro-fauna (Petterson 1996). The lack of sediment bioturbation is necessary for varve formation and preservation. More information about Gyltigesjön can be obtained from the report by Gurhén et al. (2003), in which distinct lamination in Gyltigesjön was firstly reported.

2.2 Climate regime

Westerly air flow dominates in the province of Halland, where Gyltigesjön lies. The strength of the westerlies is mainly controlled by the intensity and relative position of the Icelandic Low and Azores High (Jönsson & Bärring 1994). This atmospheric pattern can also be expressed in terms of North Atlantic Oscillation (NAO) modes. When the Icelandic Low and Azores High are intensified (NAO+), large pressure gradients will lead to strong westerly storms in north-west Europe. During periods with low pressure gradients (NAO-), cyclone tracks are positioned further south and result in weak westerly air flow (Jong 2007). Strong easterly winds do occur occasionally when a high pressure is situated over Scandinavia, causing low air temperatures in winter (Jong, 2007). The dominant westerly wind makes the climate of Halland to be mild maritime. Average temperature in January and July are -2°C and 15°C respectively. In the region of Gyltigesjön, precipitation is on average 800 to 1000 mm per year, whereas in the upland area north-east of Gyltigesjön precipitation reaches 1200 mm per year. Snow covers the area around 50 days per year. Temperature, precipitation and snow data are average values for the time period A.D. 1961–1990 (SMHI, 2011).

2.3 Deglaciation history

The Weichselian ice-margin extended more or less parallel to the coast with a north-south extension during the last deglaciation in Halland (Lagerlund & Houmark-Nielsen 1993). Påsse (1992) dated the deglaciation near Gyltigesjön to ~18000-16000 cal. yrs BP using shells from the Halland Costal Moraines (HCM). Another study (Berglund, 1995) shows this region became ice-free before 15,550-14,550 Cal. yr BP. Before the Younger Dryas (c. 10300 BP) the average regression rate was around 15-20 mm per year in this region, caused by strong glacio-isostatic rebound (Berglund 1995). A pause in the regression could have happened due to the growth of ice-mass during Younger Dryas. Subsequent rapid unloading caused the relative sea level to decrease faster. From 10,500 to 10,000 cal. yrs BP a regression up to 20 m below present sea level took place (Björck 1987). A transgression ~8 m above present sea level took place from 7,000 to 6,000 cal. yrs BP (Björck 1987). The normally recognized highest shoreline in Halland is at 60 to 70 m a.s.l (Berglund 1995).

3 Material and Methods

3.1 Coring in Gyltigesjön

In January 2010, a coring team led by Ian Snowball went to Gyltigesjön to take sediment cores for a parallel palaeomagnetic project. In order to locate the deepest part of the lake, holes were drilled through the ice-covered lake and the water depth was measured using a plumb line and a hand-held echo-sounder. A modified rod-operated fixed-piston corer (Snowball and Sandgren, 2002) was used to extract two 5-m long piston cores from two neighboring holes nearby (56°45'21"N, 13°10'34"E, Fig. 1). These two sediment cores, named GP1 and GP2, cover the sediment depth of 1.50 to 6.14 m and 3 to 8 m below the measured sediment surface respectively.

3.2 Measurement of paleomagnetic secular variations (PSV)

Sediment samples were extracted at contiguous 3-cm intervals from both GP1 and GP2 cores with ~2.2x2.2x2.2 cm^3 (7 cm^3 of internal volume) plastic boxes. Geomagnetic vectors, including direction and intensity (Fig. 2) were measured on these samples with a 2G- Enterprises superconducting rock magnetometer (SRM-755R) in the Palaeomagnetic and Mineral Magnetic Laboratory at Lund University.

Results of PSV reconstruction from GP1 is generally similar to GP2. Particularly, the relative paleomagnetic intensity (RPI) reconstructions between these two data sets show strong similarities. Due to the possibility of contamination by old soil derived carbon in bulk sediments, the limited three ^{14}C datings on bulk sediments are not sufficient to make a time-depth relationship as precise as FENNOSTACK. The PSV correlation between Gyltigesjön and FENNOSTACK was based on stretching the FENNOSTACK curve. The general pattern between these two reconstructions is very similar. This also suggests that the sediment accumulation rate in Gyltigesjön has been relatively constant over the correlated interval. The distinct easterly declination feature "f" can be correlated very well between FENNOSTACK and the palaeomagnetic data from Gyltigesjön.

3.3 Assessing the reliability of relative paleomagnetic intensity (RPI)

The strength of the geomagnetic field has been recognized as the possible influence factor for climate, which makes precise reconstruction of RPI crucial for the test of the link between the geomagnetic field and climate change (Courtillot et al. 2007; Knudsen & Riisager 2009). An ideal RPI reconstruction requires uniform magnetic properties. Variations such as magnetic mineral concentration, magnetic grain size and magnetic

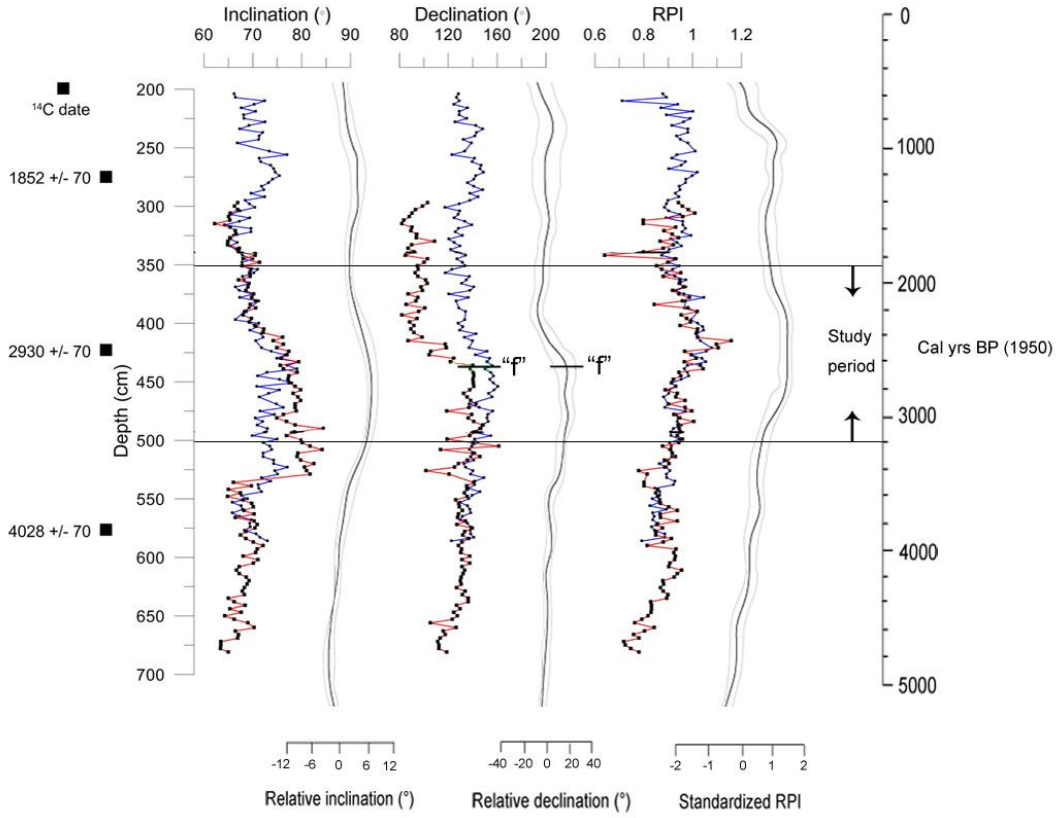

Fig. 2. *Palaeogeomagnetic reconstruction from Gyltigesjön (Data provided by I. Snowball). Inclination, declination and relative paleogeomagnetic intensity (RPI) were measured in both cores: blue-core GP1 and red-core GP2. Measurement from palaeomagnetic secular variation master curve (FENNOSTACK, black curves) and the relative palaeointensity curve (FENNORPIS, black curve) for Fennoscandia are stretched to fit with the inclination, declination and RPI measured from Gyltigesjön (Snowball et al. 2007). Easterly declination feature "f" is very distinct from the measurement in Gyltigesjön. Chronology on the right is based on FENNOSTACK. Three bulk sediments samples are dated with ^{14}C dating results listed on the left. Results of these datings are not used in this thesis. In between the two black lines is the section chosen for detailed study.*

mineralogy may influence the estimates of RPI. Tauxe (1993) concluded that the commonly measured natural remanant magnetization (NRM) does not record the true geomagnetic field strength. Influence of magnetic concentration should be considered. In this study, the RPI was calculated by using anhysteretic remanent magnetization (ARM) to normalise the NRM and correct for changes in the concentrations of magnetic minerals. Tauxe (1993) also pointed out that variations in magnetic concentration should be within only one order of magnitude and that a well-defined component of magnetization is preferred. In this case, sediment dominant by SD (smaller size) magnetite grains rather than MD (larger size) magnetite grains are better in reconstructing paleomagnetic parameters. Thus, before the comparison between geomagnetic signals and palaeoclimate data, the distribution of magnetic grain size should also be critically examined.

3.3.1 Magnetic hysteresis analysis

Parameters obtained from magnetic hysteresis loops can be used to characterize magnetic concentration, grain size and mineralogy of samples. These magnetic parameters are also sensitive to environmental change and can be used as paleoclimate proxies (Snowball et al. 1999). Sediment samples collected at 3 cm

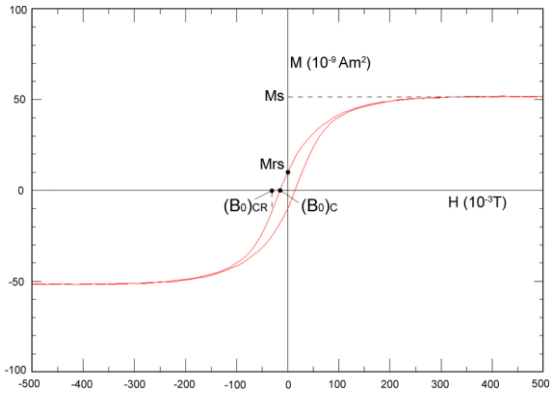

Fig. 3. *Magnetic hysteresis loop of sample GP1-306. Key values of M_s (saturation magnetization), M_{rs} (saturation remanence), $(B_0)_C$ (coercive force) and $(B_0)_{CR}$ (coercivity of remanence) are labeled.*

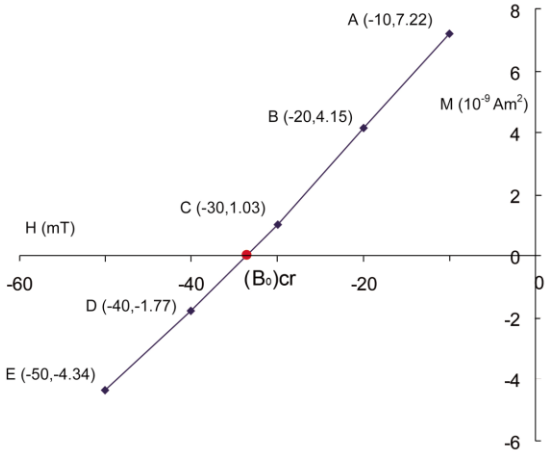

Fig. 4. *Diagram showing how $(B_0)_{CR}$ was measured. External field (H) was applied in the order of -10mT (A), -20mT (B), -30mT (C), -40mT (D) and -50mT (E). Magnetic remanence (M) after each applied field is removed can be measured with AGM-M2900-2. $(B_0)_{CR}$ is the x-value when magnetic remanence (M_r) returns to zero.*

intervals were available from cores GP1 and GP2 cores. Samples for magnetic hysteresis measurement were prepared by using an agate mortar to gently homogenize the sediments, but with care to avoid grinding (which could change the grain size distribution). After homogenization, a small amount of the sediment powder was transferred to a piece of cleaned glass and mixed with a two component epoxy resin. A wooden toothpick was used to collect glued powder and put it onto a 0.3x0.3 cm diamagnetic transparent plastic sheet before it set. To prevent samples from dust contamination in the lab, a transparent plastic box was used to cover the samples. The magnetic hysteresis properties of the samples were determined with a PMC MicroMag alternating gradient magnetometer (AGM-M2900-2). The maximum applied field (H) was set to 500 millitesla (mT). A complete magnetic hysteresis loop is obtained by cycling the magnetic field from the maximum set applied field in one direction to the same strength field in the opposite direction and back again (Fig. 3). The $(B_0)_{CR}$ (coercivity of remanence) value cannot be directly measured from hysteresis loop. The method for calculating $(B_0)_{CR}$ is shown in Fig. 4.

3.3.2 Measurement of First Order Reversal Curves

First Order Reversal Curves (FORCs) are now popularly used to represent hysteresis data (Egli et al. 2010). Unlike hysteresis loops, which characterize magnetic features with M_{rs}, M_s, $(B_0)_{CR}$, $(B_0)_C$, FORC diagrams are based on tens to hundreds of hysteresis curves and the data are graphically presented as a contour plot. Samples for FORCs analysis are the same with hysteresis measurement. In a FORC measurement, the sample is first subjected to a saturating field (1T in this study). The field is then decreased to a reversal field H_a and goes back to saturation again. One such curve, which consists of the

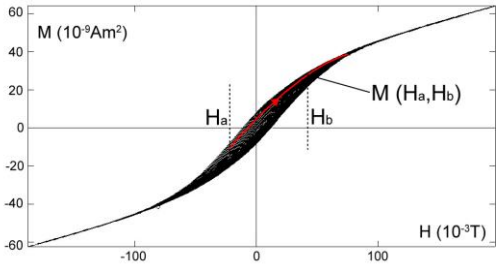

Fig. 5. *Single FORC (red line) and FORCs (clustered curves). A random point M (H_a, H_b) is labeled.*

measurement of the magnetization from H_a back to saturation, is one FORC (Fig. 5). A suit of FORCs is obtained by measuring magnetizations starting from different H_a values. With the FORCs set-up parameters used in this study it took 1.5 hours for one FORC measurement and each FORC contained 222 single reversal curves. MatLab-based program called UNIFORC was applied for further analysis and drawing of FORC related diagrams (Egli et al. 2010; Winklhofer & Zimanyi 2006).

3.4 Core correlation

One segment of Piston core GP1 (340-465 cm) and another one from GP2 (410-533 cm) were chosen for detailed analysis (easterly declination feature "f" was identified 435 cm below the sediment surface). Correlation of these two cores is based on both common varve patterns and volume magnetic susceptibility (κ, dimensionless) (Fig. 6, 7). Correlation between GP1 and GP2 is significantly high according to κ ($R^2 = 0.7141$).

3.5 Photo recording

To document sediment cores and use the photos for further analysis, images were taken with a digital camera (Nikon D80 with a AF Nikkor 60 mm 1:2.8 objective) that was mounted over the sediment cores. The sediment cores were laid down on a flat board with extra illumination provided by stable fluorescent lights (Fig. 8). Water was sprayed onto the top of the sediment to make the varves as distinct as possible (Snowball et al., 1999). A 1.5-meter long ruler was placed parallel to the sediment core on the flat board. Images were saved as JPG format with the dimension of 3872 x 2592 pixels and the resolution of 300 pixels per inch and the sediment was digitalized with the grey-scale in 8-bit. Each pixel represents a value ranging from 0 (black) to 255 (white) in the commonly used grey-scale. The following settings were made manually constant: ISO 100, white balance 5600

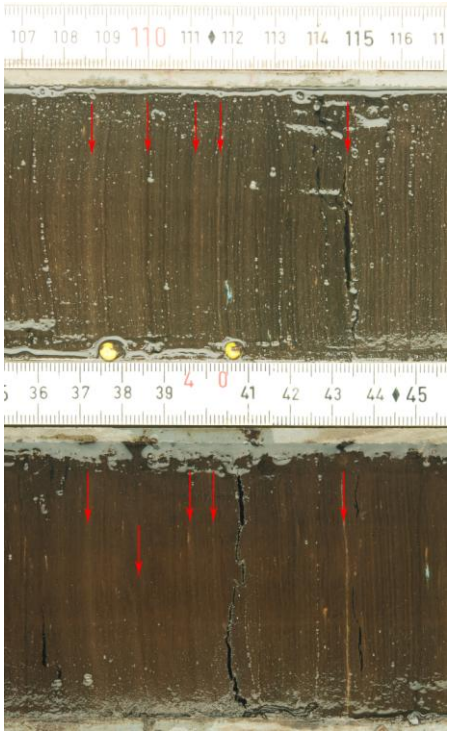

Fig.6. *Distinct common layers from GP1 (upper) and GP2 (lower) can be found and used as marker layers for correlation. Younger sediments are to the left. Photo taken by A. Johansson & W. Ning.*

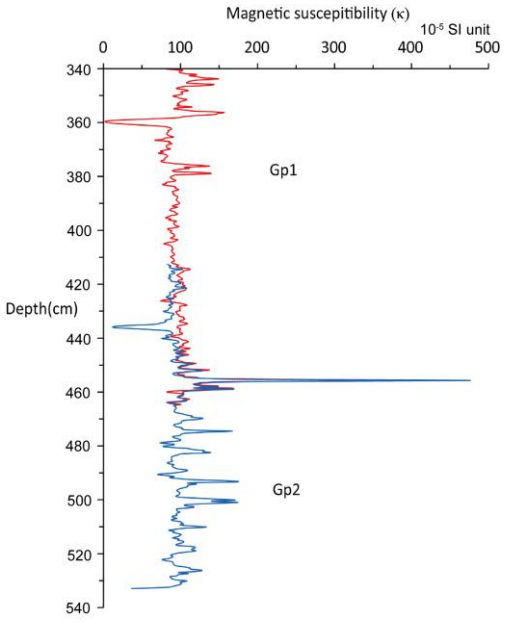

Fig.7. *Correlation between GP1 and GP2 based on volume magnetic susceptibility (κ). The distinct peak around depth 458.5 cm is caused by a common light coloured layer.*

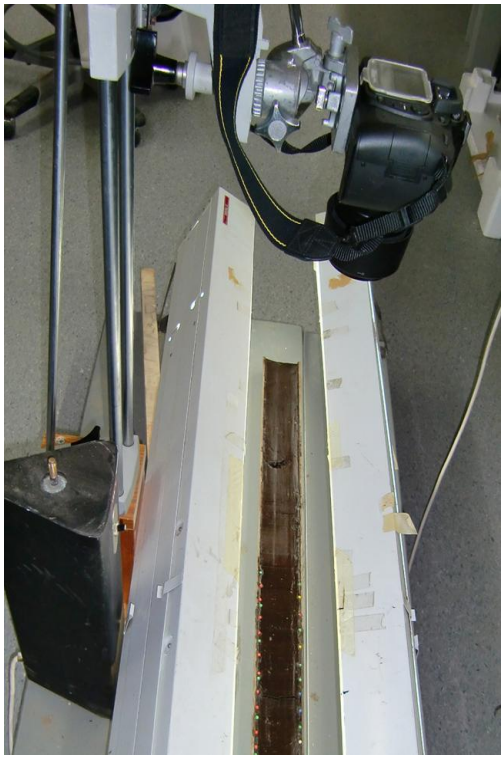

Fig. 8. *Photo illustrating how sediment is recorded by camera.*

k, aperture 8 and shutter speed 1/2 s. For each photo, about 14 cm of sediment were covered, with about 5 cm overlap with the surrounding sediment sections.

3.6 Varve counting

Since one varve represents one year, distinct features of light and dark laminas in one varve make it possible to achieve a precise chronology simply by counting the number of couplets. An age model based on varve counting can reach as far as to the time when distinct varves started to form. e.g. more than 9000 varves were counted from sediments in Kälksjön, central west Sweden (Stanton et al. 2010). The Gyltigesjön sediment surface was scraped parallel to the bedding direction of the varves with a razor blade (Snowball et al. 1999). Before counting, an appropriate amount of water was sprayed onto the sediment surface to make the varves as visually distinct as possible (Snowball et al. 1999). Varves were counted by two people alternatively under conventional microscope (Wild Heerbrugg), with the magnification between 6 and 50. LINTAB tree-ring station was used to move sediment cores horizontally. To avoid water reflections, the sediment core was slightly tilted when necessary. In order to delimit blocks of 50 years for later analyses, number of varves counted each time followed the order of 20, 20 and 10. Uncertain varves were assigned with an age error of ±0.5. For example, two people counted to different varve as the 20th (or 10th) varve, the more likely one was chosen as the 20th (or 10th) varve and the error was assigned based on the difference between the two varves. Usually a single interval was counted more than twice by each person. A pin was put aside on the 20th or 10th varve as a marker. Marker layers were also marked on photos with a red line using Adobe Photoshop® (Fig. 9).

Table. 1. *Cumulative error estimates associated with varve counting*

Total varve counted	Error estimate (±)
200	9.5
400	19
600	27
800	33.5
1000	40.5
1200	45
1400	50

3.7 Pollen analysis and vegetation reconstruction

Twenty samples with a volume of 1 cm^3 each were extracted from the sediments with a volumetric brass pollen sampler. A gap of fifty varves was placed between the centers of consecutive samples. Pollen samples were prepared according to the method described by Berglund & Ralska-Jasiewiczowa (1986). Two tablets, each containing 18,584±829 *Lychopodium* spores (an exotic marker) were added to each sample for the calculation of pollen concentrations. Samples were soaked in HF for two days in order to dissolve mineral

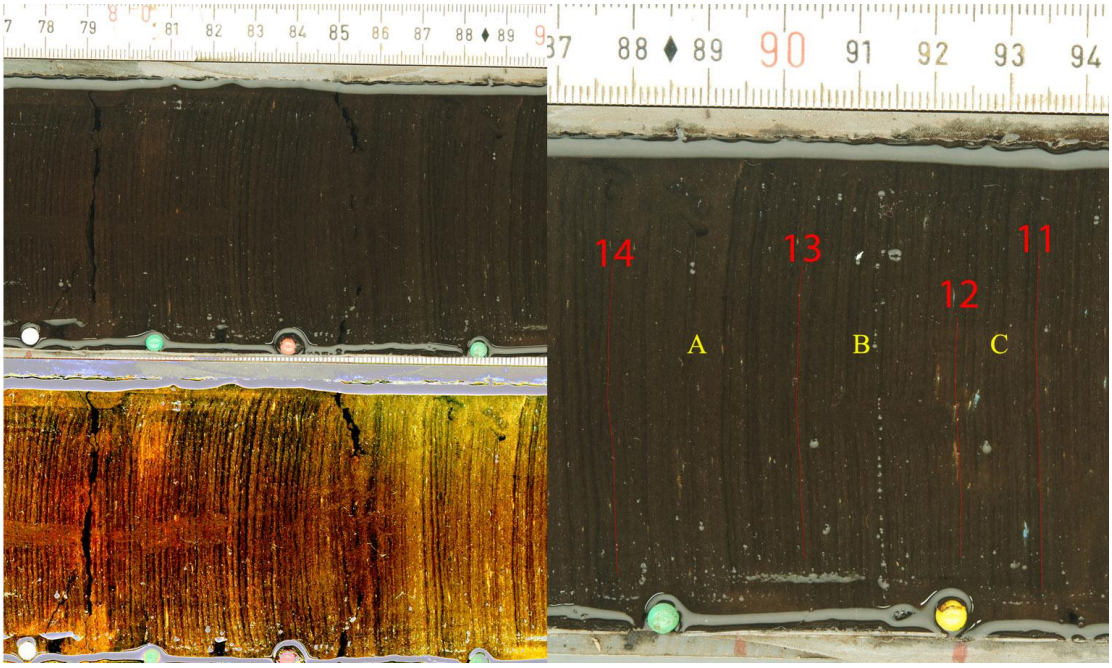

Fig. 9. *Original picture of varved sediments (upper left) and the same varved sediment after processed by Adobe Photoshop® picture of varves (lower left). Red line marks the end of intended varve number (right). Serial number of each line is labeled above the red line. For example, interval C represents 10 ±0 varves; Interval B represents 19.5±0.5 varves; Interval A represents 20.5±0.5 varves. Intended varve number for interval A, B and C are 20, 20 and 10.*

particles. To avoid counting bias, the order of samples was rearranged and kept by an independent person (A. Johansson) until all pollen samples were counted. The pollen key by Faegri and Iversen (1989) was used to identify different pollen types. Reference collection at the Department of Earth and Ecosystem Sciences at Lund University was also used to aid identification. A minimum of 500 pollen grains were identified for each slide. Both percentage and influx diagrams were constructed by using the Tilia and Tiliagraph (Grimm 1991). Zonation of the pollen diagram was constructed with CONNIS (Grimm 1987) and observation, with emphasis on the changes of wild grass pollen.

Due to differences in pollen dispersal and productivity of different taxa, pollen proportions in a sample are not linearly related to the proportions of vegetation cover on the landscape. In order to achieve a quantitative reconstruction of vegetation proportions based on fossil pollen records, a model called Regional Estimates of Vegetation Abundance from Large Sites (REVEALS) was applied (Sugita 2007). REVEALS is part of the Landscape Reconstruction Algorithm (LRA), attempting to reconstruct regional vegetation cover (10^4-10^5 km^2) from large lakes or bogs (>100 ha). The size of Gyltigesjön is not as large as 100 ha. However, when combined with the connecting lake downstream, the overall size is larger than 100 ha. In this study, REVEALS is used to estimate vegetation proportion for 26 taxa based on the Pollen Productivity Estimates (PPEs) from southern Sweden (Broström et al. 2004).

3.8 Loss on ignition (LOI)

Weights of crucibles dried at 105°C ($DW_{crucible}$, DW=dry weight) were measured and the crucibles were then arranged in order on a tray. Previous tests carried out by (Heiri et al. 2001). indicate that sample size can affect LOI results at 550 °C. To avoid this error as much as possible, sediment was weighed when put into crucibles until a certain weight close to 0.5 g was reached. Of all samples, the weights range from 0.45 g to 0.52 g (SD=0.01). Samples and crucibles were dried for 18 hours at the temperature of 105°C in

an oven and allowed to cool for a further one hour in a dessicator. The weights of sample and crucible (DW_{before}) together were measured. Subsequently the samples and crucibles were put into oven and ignited for 4 hours at the temperature of 550 °C. The weights of samples (DW_{after}) were measured after cooling for 1 hour in the dessicator. The function used to calculate LOI at 550 °C can be expressed as:

$$LOI(\%)=(DW_{before}-DW_{after})/(DW_{before}-DW_{crucible}) * 100$$

3.9 TC and Ratio of Carbon Nitrogen

The ratio of carbon to nitrogen (C/N) is commonly used as a proxy for discriminating the original source of organic matter in sediments (Meyers & Teranes 2001). Terrestrial organic matter has a C/N ratio greater than 20 whereas C/N ration of algae is only between 4 to 10 (Meyers & Teranes 2001). Samples were already ground with an agate mortar. To make fine, homogenous samples, each sample was put into a cylinder with two metal bulbs and shaken at a frequency of 30/s for 60 seconds. Each sample was weighted to the accuracy of 0.001 mg and placed in tin capsules. Air was carefully pressed out from the capsules. In total, 57 samples were prepared (mean=3.492 mg, SD=0.315 mg). Total carbon (TC) and C/N were measured with a Costech Instruments ECS4010 elemental analyser. Before measurement, five standard samples were used as calibration. Standard samples were also measured every ten samples to check the working status.

3.10 Varve thickness

Sediment photos were used for estimation of varve thickness. Before measurement, a test was made to determine if there was any significant distortion produced by the camera lens. A photo of a standard steel ruler was taken and distances of every 1 cm were measured with Adobe® Photoshop® (Fig. 10). In total, 11 1-cm intervals

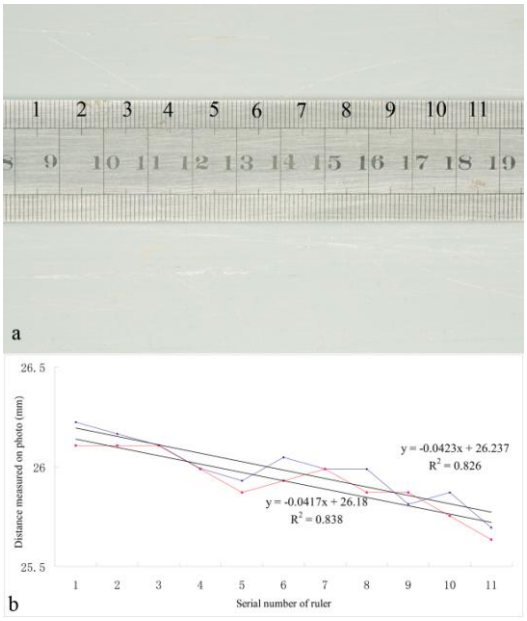

Fig. 10. *A test of lens distortion. (a) A photo of standard ruler was taken and 11 1-cm intervals were measured. (b) When plotting the distance of each interval, a linear trend can be clearly observed from the two measurements (blue and red curves).*

were measured twice. A significant trend can be observed, which can be explained by the tilting of the bent ruler towards the camera (left part of the ruler was closer to camera). A distance for 1-cm of ruler was corresponds to 25.96±0.303 (2σ) mm on the photos. Thus, error of distance measurement on photos is 1.2%, which is considered acceptable.

To estimate varve thicknesses, sediments photos taken with the 1.5-meters long ruler were used. A 1-cm interval from the 1.5-meters long ruler beside the sediment core (Fig. 9) was measured 5 times. Average distance for the 1-cm ruler was measured as 23.25 mm on photo. The thickness of varve was measured on photo and can be calculated to real thickness by dividing by 23.25 (e.g. if thickness of one varve is measured to 3 mm on photo, the real thickness of the varve would be calculated as 3 divided by 23.25, which is 0.13 cm).

3.11 Grey-scale

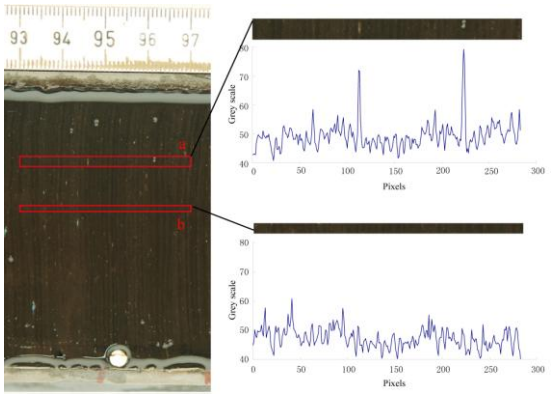

Fig. 11. *Measurement of grey scale on two continuous sections (a, b) covering the same depth. Younger sediment is to the left. Influence of water reflection and other disturbances can be very distinct on grey scale measurement.*

Grey-scales have been used to indicate the concentration of calcium carbonate in marine sediments and glacial laminations (Anderson 1996). It can also reflect changes in biogenic productivity with a darker grey representing higher concentrations of organic matter (Hughen et al. 1996). Grey-scale was measured on photos with Image J® (Fig. 11). Dimension of photos were adjusted from 3872 x 2592 pixels to 1000 x 669 pixels in order to lower data amount for processing. In this case, about 10 pixels one varve. When selecting areas for measurement, care was paid to avoid water reflections, disturbances and patches of oxidized (blue) vivianite ($Fe_3(PO_4)_2 \bullet 8(H_2O)$) . Grey scale data of GP1 and GP2 cover 113 cm and 74 cm respectively. 39 sections and 29 sections were selected as measureable areas for GP1 and GP2 respectively.

4 Results and interpretation

4.1 Floating varve chronology

In total, 1407.5 ± 50 varves from GP1 and GP2 were counted between 345 cm and 513.7 cm below sediment surface. The mean varve thickness in this interval is 1.2 mm. The original varve number-depth curve is shown in Fig. 12a. The 1408 varves can be recognized as floating varve chronology (0 to 1408 varve years). The distinct declination feature "f" identified from the PSV reconstruction makes it possible to anchor this floating varve chronology to FENNOSTACK (Fig. 2). Feature "f" is observed at 435 cm below sediment surface based on PSV reconstructions from GP1 and GP2 (Fig. 2) and its FENNOSTACK age is 2670 cal. yrs BP (Snowball, et al., 2007). Thus, the floating varve chronology (spanning 1407 years) has been secured to the FENNOSTACK timescale by assigning the 435 cm level below the sediment surface an age of 2670 cal. yrs BP. The fixed depth-age curve is shown in Fig. 12b.

4.2 Magnetic parameters and LOI

The magnetic measurements reflect the concentration of magnetic grains, size of magnetic grains and their mineralogy. Different magnetic parameters that indicate similar magnetic properties are grouped (Fig. 13) to better illustrate the magnetic properties of sediment samples (Peck et al. 2004). It is interesting to see the relationship between organic content and magnetic materials in the sediments. Thus, values of LOI result are compared with magnetic parameters.

4.2.1 Results of magnetic parameters and LOI

Measurement results of magnetic parameters and LOI are shown in Fig. 13. Four zones (A-D) are made according to common features from magnetic parameters (RPI is not included) and LOI. Correlation between each magnetic parameter is calculated and shown in Table. 2. Descriptions of the four zones are listed below.

Zone D (3220-2880 cal. yrs BP)

Zone D is the oldest period identified in this study. This zone covers ~240 years. χ and SIRM values range between 0.4 to $0.7*10^{-6} m^3kg^{-1}$ and 10 to $12*10^{-3} Am^2kg^{-1}$ respectively. The ratio of M_{rs}/M_s (0.1-0.3) is negatively correlated with $(B_0)_{CR}/(B_0)_C$ (2-3), with minor fluctuations in both ratios. $(B_0)_{CR}$ ranges between 28 and 34 mT.

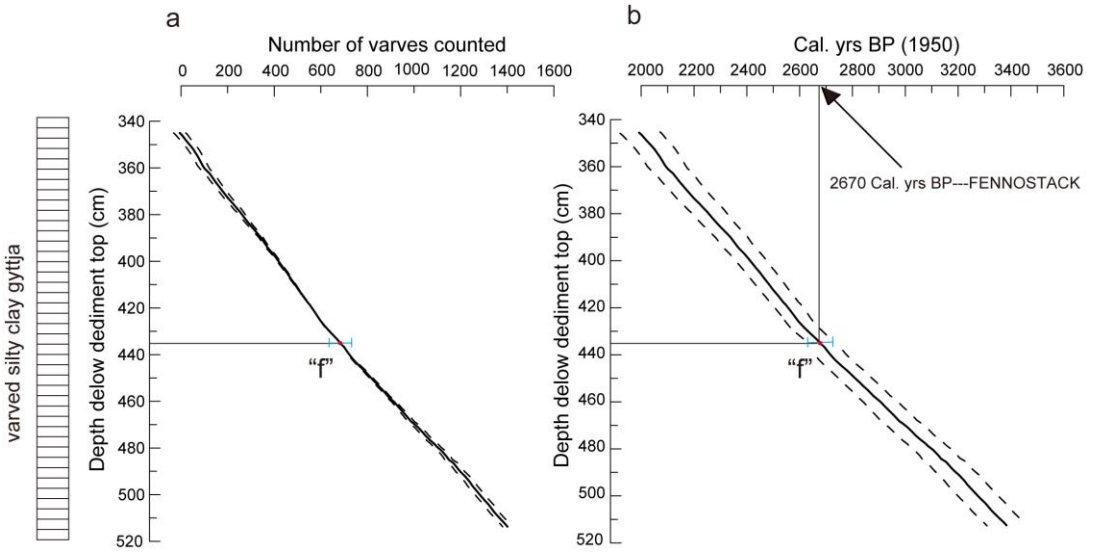

Fig. 12. *Diagrams illustrating how the floating varve chronology was anchored to the FENNOSTACK timescale (Snowball et al. 2007). The original counted varve number is plotted against the depth below sediment surface (a).Blue bar indicates the age error (±50 years) associated with feature "f" from FENNOSTACK. Doshed lines indicate the combined error from varve counting and age of feature "f" in FENNOSTACK. Filled red circle shows the depth of feature "f" based on the PSV measurement (Fig. 2). The floating varve chronology is anchored to the position of declination feature "f".*

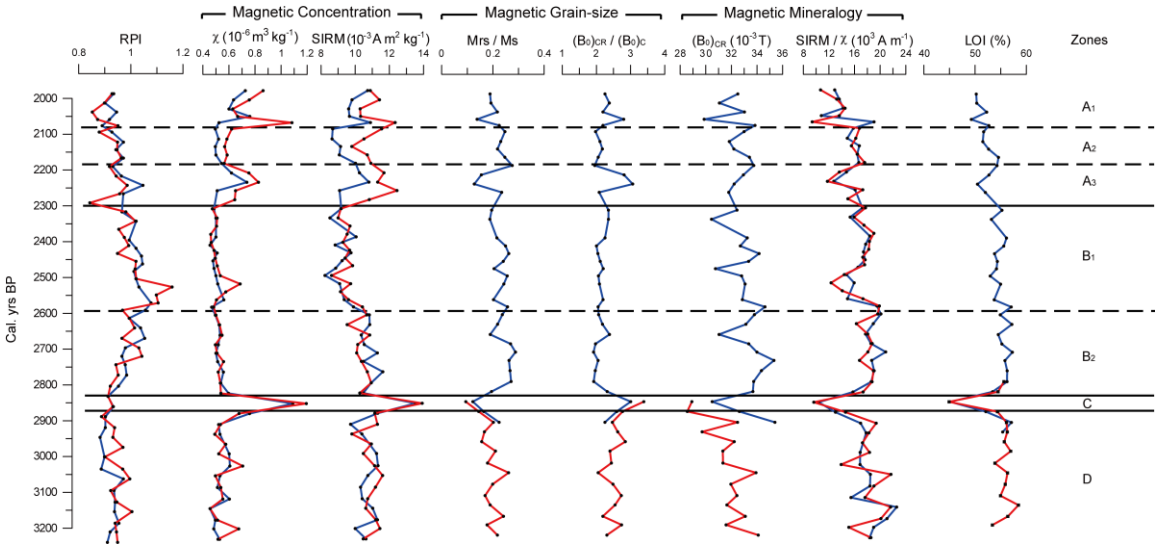

Fig. 13. *Geomagnetic relative intensity (RPI), magnetic parameters and LOI. Blue and red curves represent measurement from GP1 and GP2 respectively. Zones are separated by observation.*

Ratios of SIRM/χ lie between 12 and $20*10^3 Am^{-1}$. Values of LOI rang between 50% and 55%, showing limited variations.

Zone C (2880-2830 cal. yrs BP)

The peak in this zone is the most distinct feature from both magnetic and LOI values throughout. This zone is characterized by one unusual sample and covers 50 years. χ and SIRM values reach to their maximum at 1.2 m^3kg^{-1} and 13 $10^{-3}Am^2kg^{-1}$ respectively. Ratio of M_{rs}/M_s reaches its minimum value of 0.1 and $(B_0)_{CR}/(B_0)_C$ value reaches to the maximum of 3. $(B_0)_{CR}$ reaches its lowest value of 29 mT at this

sample. LOI reaches its minimum value of 45%.

Zone B (2830-2300 cal. yrs BP)

In general, zone B is a relatively stable phase covering 530 years. χ is generally stable in this phase, lying around $0.5*10^{-6}m^3kg^{-1}$. Dramatic decrease in SIRM values at ~2600 cal. yrs BP separate Zone B into sub-zones B_1 and B_2. SIRM values drop from 10.5 to 9.5 mAm^2kg^{-1} at this transition. This transition is not obvious in the other parameters. SIRM/χ values also decrease at this transition. Values of M_{rs}/M_s (0.2-0.3) and $(B_0)_{CR}/(B_0)_C$ (2-2.5) are stable in both sub-zones. LOI in this zone B is consistent around 55%.

Zone A (2300-1990 cal. yrs BP)

Two distinct peaks observed at 2250 and 2050 cal. yrs BP from magnetic parameters and LOI separate Zone A into three sub-zones. In sub-zone A_3 (2300-2180 cal. yrs BP), χ and SIRM reach their maximum at $0.8*10^{-6}m^3kg^{-1}$ and $13*10^{-3}Am^2kg^{-1}$ respectively. Minimum value of M_{rs}/M_s is ~0.1 and maximum value of $(B_0)_{CR}/(B_0)_C$ is ~3 in this sub-zone. These values are rather comparable with the distinct values in Zone C. Minimum of LOI is 50% in sub-zone A_3. Sub-zone A_2 (2180-2070 cal. yrs BP) is relatively stable compared with sub-zone A_1 (2070-1990 cal. yrs BP). In sub-zone A_1, highest (lowest) values of χ, SIRM and $(B_0)_{CR}/(B_0)_C$ (M_{rs}/M_s) are all rather distinct when compared with values from the whole sequence. These distinct values are measured from one sample, which characterizes sub-zone A_1. Zone A is the most variable phase of all zones.

4.2.2 Interpretation of magnetic parameters and LOI

χ and SIRM are recognized as parameters reflecting magnetic concentration (Snowball et al., 1999). χ is generally recognized as indicator of ferrimagnetic mineral concentration. If there is limited amount of ferrimagnetic minerals (eg. magnetite) in a sample, abundant diamagnetic material such as organic matter and quartz will have a strong dilution effect and reduce χ values, possibly to negative values. SIRM is primarily a measurement of ferrimagnetic mineral concentration as well. However, grain size and mineralogy can influence SIRM value as secondary factor. Correlation between χ and SIRM (r=0.67) is the lowest if compared with correlation between χ and all the rest parameters, including LOI. This means that there must be other factors other than concentration affecting SIRM values, such as grain size and/or mineralogy. Ratios such as M_{rs}/M_s and $(B_0)_{CR}/(B_0)_C$ indicate the domain state of ferrimagnetic minerals, which can be used as a proxy of physical grain size (Dunlop 2002). Correlation between M_{rs}/M_s and $(B_0)_{CR}/(B_0)_C$ is very high in this study (r= -0.95). Lower (higher) M_{rs}/M_s values and higher (lower) $(B_0)_{CR}/(B_0)_C$ indicate coarser (finer) magnetic grains. SIRM/χ

Table. 2. Correlation coefficient between RPI, magnetic parameters and LOI.

	RPI	χ	SIRM	M_{rs}/M_s	$(B_0)_{CR}/(B_0)_C$	$(B_0)_{CR}$	SIRM/χ	LOI
RPI	1							
χ	-0.32	1						
SIRM	-0.32	0.67*	1					
M_{rs}/M_s	0.27	-0.71*	-0.40*	1				
$(B_0)_{CR}/(B_0)_C$	-0.27	0.74*	0.52*	-0.95*	1			
$(B_0)_{CR}$	0.22	-0.5*	-0.15	0.74*	-0.66*	1		
SIRM/χ	0.21	-0.78*	-0.08	0.65*	-0.56*	0.53*	1	
LOI	0.23	-0.80*	-0.22	0.56*	-0.51*	0.47*	0.88*	1

**** significant correlation at 99% level***

is partly an indicator of grain size as well, but requires the presence of only one kind dominating ferrimagnet. Higher value of SIRM/χ means finer grain size, although extremely high values could indicate the presence of the iron sulfide mineral greigite (Snowball, 1999). $(B_0)_{CR}$ is primarily an indicator of grain size. Lower $(B_0)_{CR}$ values indicate larger magnetic grain size. $(B_0)_{CR}$ can also be used as mineralogy indicator of magnetic mineral (e.g., $(B_0)_{CR}$ of hematite, goethite and greigite are high). LOI values indicate the amount of organic content in a sample. Low values of LOI could be caused by high input of clay or sand, this is supported by the negative relationship between LOI and χ (r=-0.8).

Results of $(B_0)_{CR}$ and SIRM/χ both indicate magnetite as the dominate magnetic mineral in the sediments throughout (Thompson & Oldfield 1986). Highest values of both SIRM and χ at 2850 cal. yrs BP (Zone C) indicate that there is a large input increase of magnetic minerals at this time. The size of these grains is relatively large as well based on low value of M_{rs}/M_s and high value of $(B_0)_{CR}/(B_0)_C$. Since these unusually high values are only created by one sample, this event must be short in time (50 years) or the measurement is an outlier. In fact, it is possible that the erosion event only lasts one or several years based on observation of the lithology (only one distinct sandy lamina observed). This event could be related to high precipitation, storm or human activity associated with land use change. It is difficult to conclude whether the transition of sub-zone B_1 and B_2 (2600 cal. yrs BP) is a significant change. Only SIRM shows significant decrease at this time whereas χ, grain-size indicators and LOI show limited changes. In general, Zone A is a quite variable phase with intense erosion around Gyltigesjön. During this time, higher amount of magnetic minerals, both fine and coarse, were transported into the lake. Similar to Zone C, it is very likely the two distinct erosion events in Sub-zone A_3 (2250 cal. yrs BP) and A_1 (2050 cal. yrs BP) are created by intense precipitation events or by intensified human activity.

4.3 Assessing the reliability of RPI

4.3.1 Correlation between RPI and magnetic parameters

To examine whether any magnetic parameter has significantly influenced the RPI reconstruction correlation coefficients were calculated between RPI and each magnetic parameter (Table. 2). Correlation coefficients between RPI and other parameters are all very low and not significant at the 99% confidence level. This indicates that no single parameter has dominated the signal of RPI estimation. According to Tauxe (1993), sediment with limited magnetic concentration variation (less than one order) is preferred for paleomagnetism reconstruction. It is obvious sediments in Gyltigesjön conform to the criteria for valid RPI. Basically, there is no statistically significant evidence of environmental bias of the RPI reconstruction.

4.3.2 Magnetic hysteresis data and Day plot

The so-called Day plot is usually used to study magnetic grain sizes (Day et al., 1977). The Day plot in Fig.14 displays the magnetic hysteresis properties of sediment samples in different zones. Grains of different sizes will show different magnetic hysteresis fingerprints, capturing different zones (SD, PSD and MD) in the M_{rs}/M_s versus $(B_0)_{CR}/(B_0)_C$ diagram. Result of Day plot shows a spread of points spanning the pseudo-single-domain (PSD) grain size range. The PSD status can be recognized as a transitional status between MD and SD statuses. It is not proper to interpret these magnetic grains as PSD because mixture of SD and MD grains could also show such distributions. Given the fact that SD magnetite grains can be created by magnetic bacteria in Sweden (Snowball, 1994), it is possible that magnetic grains in the sediment samples actually have a bimodal grain

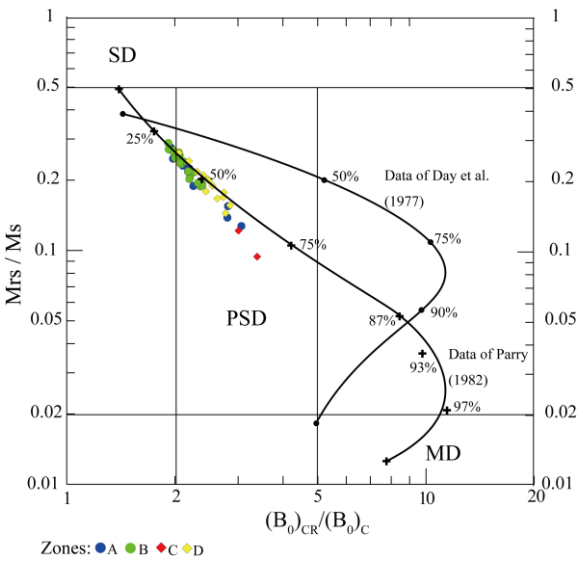

Fig.14. *Day-plot of samples showing the hysteresis properties of samples from the four zones (A-D). Experimental data for bimodal mixtures of magnetite and titanomagnetite grains from Parry (1982) and Day et al. (1977) are plotted. Percentages are volume fractions of coarse MD grains in each mixture.*

size distribution. This bimodal distribution of multi-domain (MD, larger size) grains originating from catchment erosion and single-domain (SD, smaller size) grains produced in lake, is also proposed by Stanton (2011) based on a similar palaeomagnetic study of biogenic/clastic varves in another Swedish lake. The distribution of the samples shows a similar trend with (Parry 1982) curve of bimodal mixtures of magnetite and titanomagnetite grains (Fig. 14), which further supports the bimodal interpretation. Even though, without further knowledge about the interaction of neighboring grains, the percentage labeled in Fig.14 cannot be directly used for samples in Gyltigesjön.

Hysteresis properties of samples in Zone D (3220-2880 cal. yrs BP) are relatively scattered in the Day plot, indicating a rather variable condition. Samples in Zone C (2880-2830 cal. yrs BP) obviously contain the highest proportion of MD grains, indicating a rather intense erosion event at 2850 cal. yrs BP. Composition of coarse MD grains in Zone B (2830-2300 cal. yrs BP) is very low. The variation of grain sizes is very limited as well. Grain sizes of samples in Zone A (2300-1990 cal. yrs BP) are very variable. This very scattered feature could imply a period with intense erosion events, which is consistent with the interpretation in section 4.2.2. The majority of samples are, however, clustered in the areas implying high concentration of SD grains, which indicates the samples are very good to reconstruct paleomagnetic intensity.

4.3.3 FORC diagram

Since SD, PSD, and MD grain sizes each produce different FORC contours, the FORC diagram is becoming popularly used to better resolve the mixed character of magnetic mineral samples than Day plots alone (Egli et al. 2010; Roberts et al. 2000; Winklhofer & Zimanyi 2006). Of the three samples analyzed with UNIFORC, sharp and narrow central ridges can be observed from all of the three FORC diagrams. All of these FORC diagrams are characterized by relatively closed contours along the Hc axis and a narrow spread along the Hb axis. These two characteristics imply that non-interacting SD grains or non-interacting chains of magnetite (possibly magnetosomes) are the dominant content in the samples (Michael Winklhofer, personal communication). Besides, these FORC diagrams are very similar to those obtained from a lake sediment sample known to contain bacterial magnetite (Egli et al. 2010). Bacterially-produced magnetite is believed to be the main carrier of natural remanence in some Swedish lakes (Snowball, 1994; 1999). However, without identification of bacterial magnetosome or chains from Transmission Electron Microscopy (TEM), the precise origin of the abundant single-domain magnetic grains in Gyltigesjön remains unknown. GP1-329 is a sample that can contain a high proportion of coarse MD grains (Zone C), based on interpretation from Day plot (Fig. 14). The strength of the signal is not as strong as the other

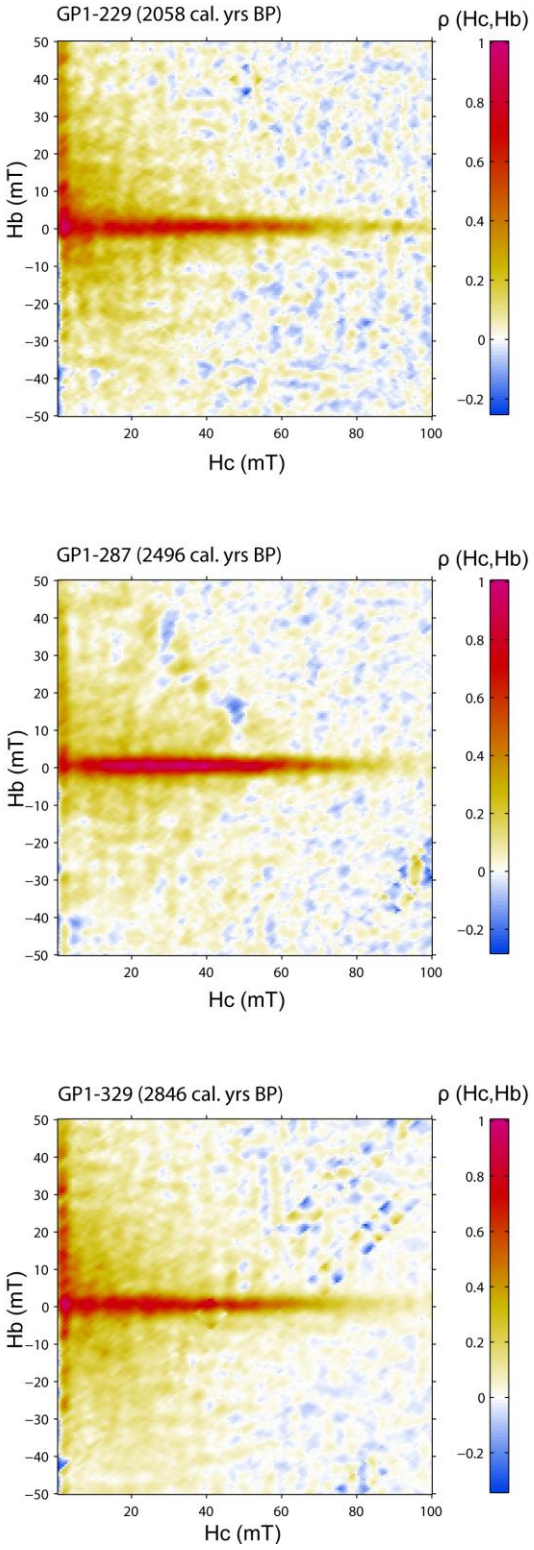

Fig. 15. *FORC diagrams of three samples GP1-229, GP1-287 and GP1-329. Smoothing factor is set to 3 (SF=3) in UNIFORC. Note the one order of magnitude difference between the amplitude of the central ridge and the remaining part of the diagram.*

two, but it is still characterized by a sharp and narrow central ridge similar to the other two samples in FORC diagram. To sum up, the FORC analyses indicate that non-interacting SD grains or non-interacting chains of magnetite are the dominant magnetic grains, which are ideal for RPI reconstructions.

4.4 Pollen stratigraphy and vegetation development

4.4.1 Results of pollen analysis

Pollen analysis is a well established method to study paleoenvironments and to reconstruct past human activities (Björkman 2001; Jong 2007). Results of the pollen analysis, including percentage, influx data and the predictions of the REVEALS model are shown in Fig. 16, 17, 18. For reliable reconstruction of vegetation proportion with REAVEALS, at least 1000 pollen grains of the defined taxa should be counted (Sugita 2007). The minimum amount of 1000 grains is not reached in this study. Thus, there must be relative larger error for REVEALS result. In general, pollen of trees and shrubs are dominant, making up to 90-95% of all pollen. This corresponds to 80-90% vegetation cover of trees and shrubs according to the REVEALS model. Composition of herbs is generally low (<5% of pollen percentage) and stable. Proportion of wild grass is 8-20% based on REVEALS model, with several periods of significant changes. *Plantago lanceolata*, *Rumex acetosa*, *Artemisia*, *Chenopodiaceae* and *Compositae cichorioideae* are grouped as indicators for human activity. The pollen stratigraphy is divided into two pollen zones (I, II) with two sub-zones each, based on cluster analysis and observation. Descriptions of pollen zones are listed below.

Zone I-1 (2960– 2880 cal. yrs BP)

This zone contains only two counted samples. *Betula*, *Pinus*, *Alnus*, *Quercus* and *Corylus* are the dominant tree species, taking up to more than 90% of total pollen. Percentage of *Gramineae*

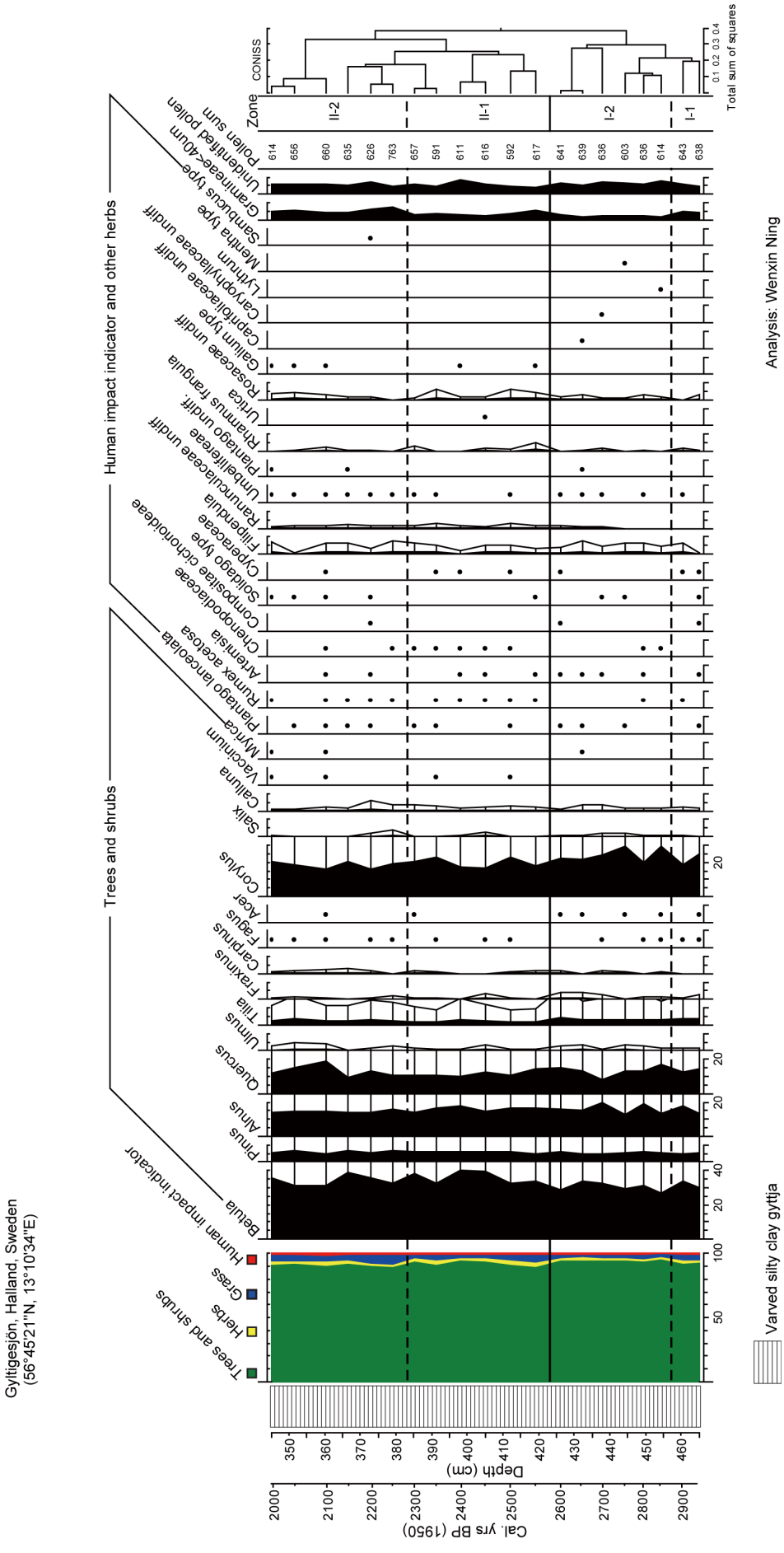

Fig. 16. *Pollen percentage diagram from Gyltigesjön. Percentages lower than 0.5 % are shown as black dots. All the identified species are shown in the pollen percentage diagram. Black curves show the exaggeration of 5 times.*

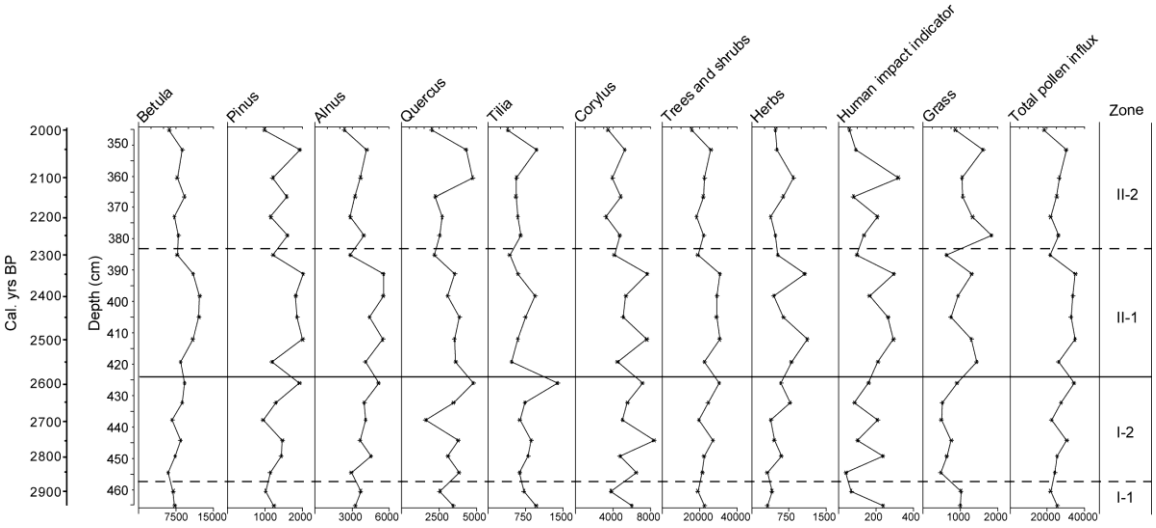

Fig. 17. *Pollen influx for main vegetation species identified in Gyltigesjön. Number below each species indicates pollen amount per cm^2 per year in the lake sediment.*

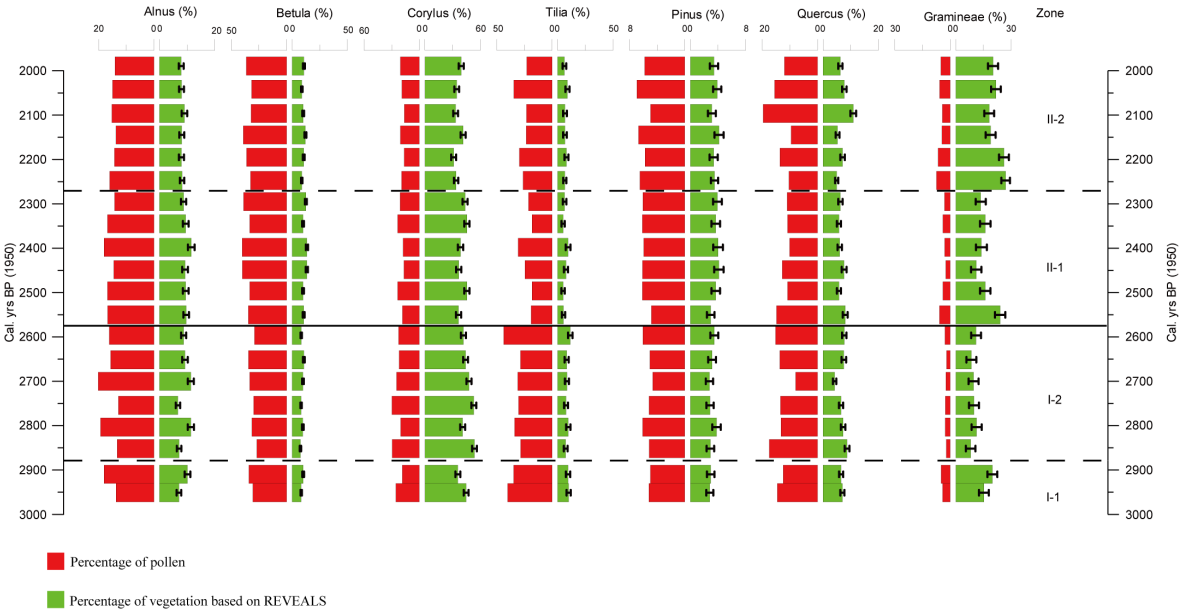

Fig. 18. *Modeled proportion of vegetation cover (green) by REVEALS and the original percentage of pollen (red).*

pollen is as 5%, corresponding to 15% of total vegetation cover according to REVEALS model.

Zone I-2 (2880– 2580 cal. yrs BP)

All the three pollen diagrams suggest that around 2880 cal. yrs BP, *Gramineae* and *Alnus* decrease and *Corylus* increases. Percentage of *Gramineae* is very low and stable, taking up ~12% of total vegetation cover (~3% of total pollen). According to the REVEALS model, the regional vegetation composition is generally stable in this zone, with *Alnus* ~8%, *Betula* ~10%, *Corylus* ~50%, *Tilia* ~10%, *Pinus* ~2.5%, *Quercus* ~8%. Percentage of *Betula*, *Pinus*, *Alnus* and *Quercus* are more stable than Zone I-1. In general, variation within this zone is very limited.

Zone II-1 (2580– 2270 cal. yrs BP)

Trees and shrubs slightly decrease at this time whereas percentage of herbs and grass increase slightly. This change is obviously observed at the transition from Zone I to Zone II. This

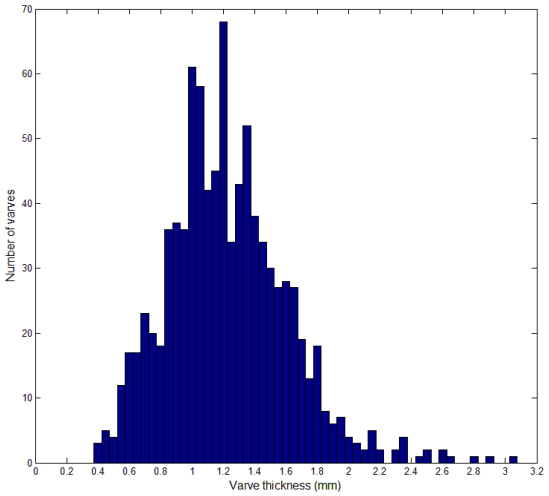

Fig. 19. *Histogram illustrating the distribution of varve thickness.*

feature can also be observed from pollen influx diagram. In addition, the REVEALS model shows *Tilia* decreases from ~10% to ~5% of total vegetation cover and the proportion of *Gramineae* increases from ~10% to ~20%. Although a slight decrease of *Gramineae* took place 2460 cal. yrs BP, wild grass is still more common in Zone II than Zone I, based on both percentage and influx diagram.

Zone II-2 (2270– 1990 cal. yrs BP)

Around 2270 cal. yrs BP, trees and shrubs decreased sharply based on pollen percentage and influx diagrams. Influx of wild grass increased to its maximum (1800 grains per cm^3) shortly after 2300 cal. yrs BP. This corresponds to 20% of total vegetation cover based on REVEALS model. Shortly afterwards trees and herbs decreased to their minimum, they seemed to increase to a stable level afterwards. Interestingly, this pattern seems very similar with Zone II-1. This pattern is also very obvious from the REVEALS model of grass reconstruction.

4.4.2 Interpretation of the pollen data

Low proportion of human-impact indicators and the absence of secale cereal pollen (cultivation indicator) imply that there was limited human activity going on in the lake catchment during the 1st Millennium BC. As relative large lake, it is believed that pollen reconstruction from Gyltigesjön can reflect a regional vegetation condition covering even the coastal area (Fig. 1). Thus, settlement in this region would be very sparse at that time. Although rare, sporadic finds of *Plantago lanceolata*, *Artemisia*, *Rumex acetosa*, *Chenopodiaceae*, *Compositae cichorioideae* and *Umbelifereae* seem to indicate that humans did leave a regional fingerprint, but at a low level of disturbance.

The decrease of trees and the increase of grass at 2580 cal. yrs BP imply that the landscape started opening up at that time. Continuous increase of human-impact indicators implies that the landscape opening was human-induced. The subtle pollen influx decrease of trees and shrubs indicate that the opening could be weak. At 2270 cal. yrs BP, proportion of grass increases distinctly. Influx of trees and shrubs is very low at this time. These could imply that a more intense human activity (possibly deforestation) was going on. However, influx of human-impact indicators does not show a significant increase. On the contrary, it stays at a rather low level.

Human activity seems to be the plausible cause for the changes in pollen records, especially the wild grass changes. Even though, climate variations cannot be ruled out from the available data.

4.5 TC, C/N, varve thickness and grey scale

4.5.1 Results of TC, C/N, varve thickness and grey scale

TC values are linearly correlated to LOI and the relationship between these two parameters can be expressed as: TC=0.45*LOI+1.6 (R^2=0.9). The most distinct difference between LOI and TC can be observed at 2560 cal. yrs BP, where a larger amplitude decrease in TC is observed. Ratio of C/N ranges from 16 to 18, with the

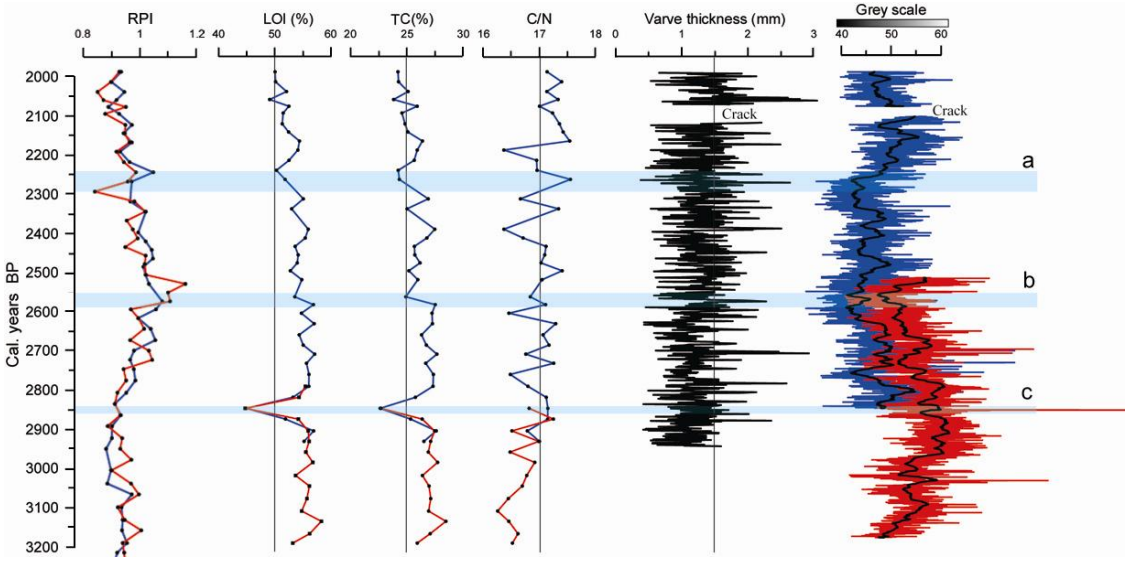

Fig. 20. *Results of LOI, TOC,C/N, varve thickness and grey scale. Blue and red curves are derived from GP1 and GP2 respectively. Trend line for grey scale is based on running average of 100 pixel values.*

Table. 3. Correlation coefficient between listed proxies

	LOI	TC	C/N	Varve thickness	Grey scale
LOI	1				
TC	0.96*	1			
C/N	-0.40	-0.53*	1		
Varve thickness	-0.25	-0.24	0.08	1	
Grey scale	-0.37	-0.29	0.27	0.34	1

**** Significant correlation at 99% level***

average value of 17 (Fig. 20). Values of C/N are generally low before 3000 cal. yrs BP and constantly high after 2150 cal. yrs BP. The lowest value and highest value of C/N occur 3120 cal. yrs BP and 2250 cal. yrs BP respectively. TC is significantly correlated with C/N (r=-0.53) at 99% level (Table. 3). The distribution of measured varve thickness is shown in Fig. 19. Majority of varve thickness is between 0.8 and 1.6 mm. Minimum and maximum varve thickness's is 0.38 and 3.05 mm, respectively (Fig. 20). Majority of grey scale values range between 40 and 60. Higher values indicate lighter colour sediments. 42-cm sediment overlap of GP1 and GP2 is measured, coving from 2500 to 2850 cal. yrs BP. The general patterns of grey scale values from the overlap are similar with each other. However, values of grey scale are consistently higher in GP2 than GP1. Grey scale is not significantly correlated with any of the other parameters (Table. 3).

4.5.2 Interpretation of TC, C/N, varve thickness and grey scale results

Higher values of C/N imply a higher content of terrestrial organic material, which could be due to the increase of terrestrial vegetation or stronger soil erosion in the catchment area. Thickness of clastic varves in northern Sweden has been found to be linked with precipitation (Wohlfarth et al. 1997). However, thickness of the biogenic/clastic varves can not simply be controlled by precipitation. It is believed that changes of lake productivity (eg. diatom assemblage), land use, erosion and climate variations in the lake catchment (eg. agricultural) can all influence the varve thickness, making

thickness of such biogenic/clastic varves hard to interpret. Low correlations between grey scale and other proxies make it difficult to interpret which environmental parameters determine the grey scale data (a 30-pixels running average of grey scale values from GP1 is used to calculate the correlation coefficient). In general, more organic matter would result in darker sediment. The almost constant difference between GP1 and GP2 on grey scale could be produced by differences of storage condition or photo taking (different amount of water on the sediments surface from GP1 and GP2). This makes the explanation of grey scale even more difficult. Another study by (Dean et al. 2002) also shows that grey scale values from lake sediments are difficult to interpret. They assumed that grey scale could possibly relate to variations in biogenic silica (diatoms), authigenic $CaCO_3$, several authigenic iron and manganese minerals. Although some proxies are difficult to interpret here, distinct changes of these proxies can possibly related to variations either to climate or human impact.

There are three relatively short phases (a, b and c) observed when all the proxies are combined (Fig. 20), which appear to record abrupt environmental changes. Phase c probably represents an intense catchment erosion event, which is already found through the magnetic parameters (Fig.13) and this interpretation is supported by the relatively high value of C/N. The varve thickness increased, most likely due to the greater input of clastic material. Pollen analysis also implies that human activity is responsible for this event. Phase b represents a transitional phase. The decrease of organic material proportion and increase of varve thickness could indicate a phase with high erosion as well. The timing of this transition is consistent with the increase of wild grass pollen and decrease of trees and shrubs pollens (Figures 16 and 17), making human activity a likely cause for this change in vegetation cover. Phase a is characterized by a decrease of LOI and increase of C/N, indicating a period with high catchment erosion. Grey scale values increase dramatically as well, which could be due to higher input of clastic material but, as stated earlier, the interpretation of this parameter is complicated. Compared to Phase b, magnitude of the erosion in Phase a is larger. This higher magnitude can also be observed from pollen analysis.

5 Discussion

5.1 Assessment of the link between geomagnetic field behavior and reconstructed climate changes

Direct comparisons between RPI and climate proxies derived from Gyltigesjön (Fig. 13, 16, 20) imply that there is no significant correlation between these two factors for the 1st millennium BC. Subtle changes recorded from several proxies (Figures16, 17 and 20) indicates that human activity is responsible for the subtle changes at 2580 and 2320 cal. yrs BP (possibly the erosion at 2850 cal. yrs BP as well), rather than natural climate variability. Further studies of early human activity in the study area are needed to better evaluate the level of human impact and this will be discussed in more detail in the following section. The distinct erosion event at 2850 cal. yrs BP, confirmed by multi-proxies (Fig. 13) does correspond with a phase of low geomagnetic field intensity. However, this correlation is only based on one sample, which makes it like a coincidence and there is a possibility that the palaeomagnetic properties of this sample have been affected by environmental bias.

5.2 Age of feature “f”

The accuracy of the age-depth model in this thesis is, to a high degree, determined by the FENNOSTACK age assigned to feature “f”. The age of the feature “f” in FENNOSTACK (2670

cal. yrs BP) is determined by a combined varve chronology obtained from six independent varve chronologies in Fennoscandia and the estimated error associated with the independent varve chronologies is ~50 years (I. Snowball, personal communication). To compare the results of RPI and climate proxies in this study to other studies, the reliability of the age of feature "f" must be assessed.

By validating a Swedish varve chronology using radiocarbon, paleomagnetic secular variation, lead pollution history and statistical correlation, Stanton et al. (2010) dated the age of feature "f" to 2650 cal. yrs BP (unknown error), which is within the errors of FENNOSTACK. Stanton et al. (2010) compared their corrected varve chronology to 12 calibrated bulk sediment radiocarbon determinations and determined the variable contamination (reservoir) effect brought by input of old carbon from bedrock and soil in the lake catchment of Kälksjön to be ca. 300-550 years around 3000 cal. yrs BP. A so-called ^{14}C wiggle-match of feature "f" in Gyltigesjön (A. Johansson, unpublished), which is based on 14 densely spaced ^{14}C datings on bulk sediments (sample for the dating is the same with pollen analysis) indicate that the age of feature "f" is between 2732 and 2683 (2σ) cal. yrs BP, with the average of 2710 cal. yrs BP, which lies within the error of FENNOSTACK. (Fig.21). The radiocarbon reservoir age for the wiggle-match period is ~300 years based on A. Johansson's dating result (Fig. 21). Lead pollution dating of sediment in Gyltigesjön by (Gurhén et al. 2003) shows that at the depth of 350 cm below sediment surface, the age is 2000 cal. BP. This age-depth relationship corresponds well to the FENNOSTACK based PSV chronology applied to this thesis (Fig.12b). However, the coring site and method used by Gurhén (2003) might have been different from this study, which could result a different age difference. For example, a 10-cm offset in depth estimation corresponds to a ca. 80-year.

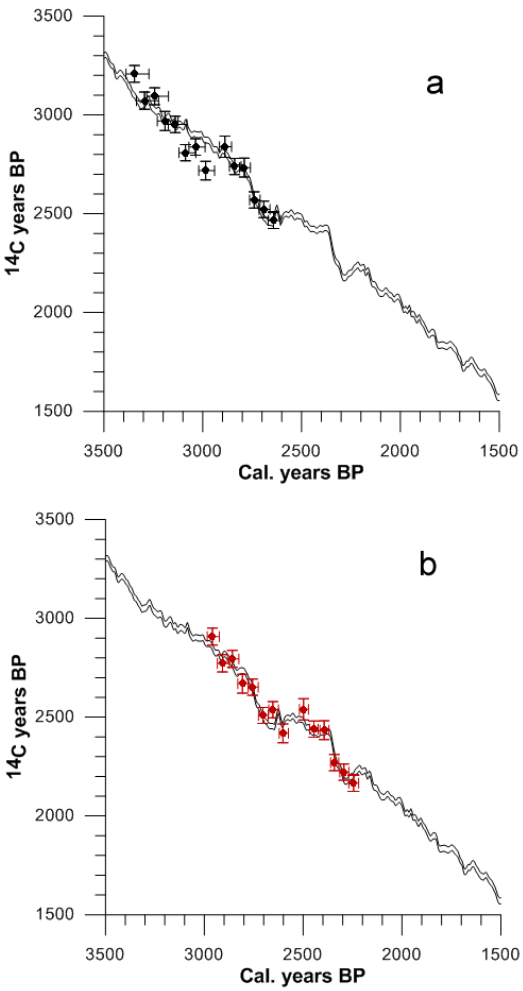

Fig. 21. *(a) The black symbols represent the preliminary radiocarbon dating results on the 14 bulk samples (A. Johansson, unpublished) from sediments in Gyltigesjön. (b) The red symbols represent the wiggle-matching results with the best model fit. Compared with preliminary dating from (a), a 300-years (^{14}C years) reservoir age is acquired (A. Johansson, unpublished).*

Differences in the palaeomagnetic "lock-in" delay in different lakes, and different sampling resolutions for PSV reconstruction can also cause age discrepancies for feature "f" (Stanton 2011). So far, for the dating results of feature "f", the radiocarbon wiggle-match can be considered to be the most reliable, indicating that the age of feature "f" is 2710 cal. yrs BP. Compared with FENNOSTACK, this age is about 40 years older, but it does remain within the error of FENNOSTACK.

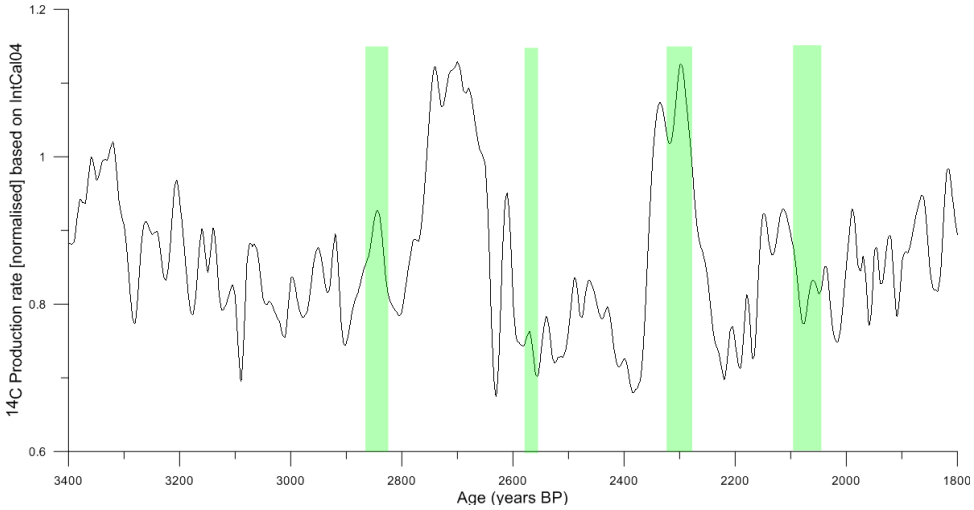

Fig. 22. *Timing of significant environmental disturbances in this study (green bars) and the ^{14}C production rate. High values of ^{14}C rate indicate period with low solar activity.*

5.3 Human impact or climate change?

To detect whether solar induced climate change or human activity caused the environmental disturbances in the lake catchment, ^{14}C production rates as a index for solar activity and the timing of significant disturbances in this study are compared to each other (Fig. 23). There are two periods of sharp decline of solar activity observed in the ^{14}C production rate, which are 2800-2700 years BP and 2380-2300 years BP. It is interesting that the environmental disturbance around 2300 cal. yrs BP correlates with one of the solar decrease. When using the radiocarbon wiggle-match based date, which uses the same calendar year timescale, the disturbance around 2300 years BP can be matched with the period of low solar activity. However, the pollen influx data show that the amount of trees and shrubs does not recover after this presumed period of cooling, which implies that intense human induced deforestation is a better direct explanation of the vegetation changes than a short period of climate cooling.

Pollen study on apophytes (i.e. shrubs, herbs and graminids favoured by man) and anthropogenic species (i.e. herbs and graminids introduced by man) from Gyltigesjön indicates that there was no large scale human disturbance in this area until about 1200 BP (Gurhén et al., 2003; 2007). Diatom inferred lake-water pH increased as a result of agricultural land use around Gyltigesjön at 1200 cal. yrs BP simultaneously with the emergence of anthropogenic species, which further confirms the timing of early regional human activity (Gurhén et al. 2007). However, the time studied by Gurhén et al. only covers the latest 2000 years.

Reconstruction of human activity based on pollen analysis from a peatland on Kullaberg, 72 km to the south-west of Gyltigesjön, showed that there could be human activity already going on as early as 3500 cal. yrs BP, although significant human activity was not found until around 1300 cal. yrs BP (Björkman 2001). Another study shows that a significant increase in landscape openness was recorded at two bogs (Undarsmosse and Store Mosse) in Halland at the Bronze Age–Iron Age transition 3000 cal. yrs BP (de Jong 2007). Based on these studies, humans were active in Halland as early as 3000 cal. yrs BP, but significant human impact started ~1300 cal. yrs BP.

These earlier studies suggest that humans were active during the period covered by this study. The pollen analysis, LOI and varve thickness etc. made as part of this study seem to support this conclusion, with significant changes

now dated to 2580 and 2320 cal. yrs BP. The pollen data from Gyltigesjön is consistent with this pattern, with stronger expansion human activity around 2580 and 2320 cal. yrs BP. The pollen data imply that human activity becomes more intense in a stepwise manner, which is similar to the expansion pattern in north-west Europe for the last 6000 years recorded by(Berglund 2003). Though limited, the subtle impact of human activity on the landscape and its effect on the physical properties of the sediments in Gyltigesön make it very difficult to find evidence of a link between climate and geomagnetic intensity.

5.4 Compare with the study of Undarsmosse

Aeolian sediment influx (ASI) result from Undarsmosse (Jong 2007) is compared with results of LOI , total pollen influx and wild grass influx in this study. The intense erosion at 2850 cal. yrs BP does not correlate to a high ASI value. This implies this erosion event is very local and not likely related to strong storm. The peak of ASI at 2580 cal. yrs BP correlates very well with the increase of grazing and decrease of pollen influx in this study. Direct comparison of land use records (cultivated and grazing) with ASI in her study, de Jong (2007) found that as agricultural areas expanded after 3000 cal. yrs BP, the amplitude of ASI peaks increased. De Jong (2007) argues that as the landscape opened up, the increase of sediment availability made the sand influx values increase. She claimed that ASI values were significantly related to human activity for the latest 1500 years. Thus, the correlation between the ASI peak and pollen analysis provides additional evidence that human activity started to become more intense at this time. When the wild grass flux increases, the ASI values increase as well (Fig. 23). This correlation indicates that human activity could have influenced the ASI values as early as from 3000 cal. yrs BP.

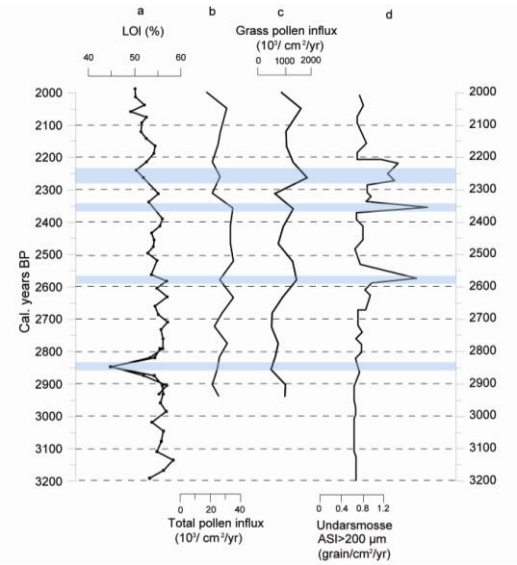

Fig. 23. *LOI (a), total pollen influx (b) and wild grass pollen influx (c) derived from Gyltigesjön. Aeolian sediment influx (ASI)* (d) *is based on grains larger than 200 µm (de Jong 2007).*

5.5 Geomagnetic field and solar activity

There is a hypothesis that Earth's climate could be affected by changes in cloudiness caused by variations in the amount of galactic cosmic rays (GCRs) arriving to the atmosphere (Carslaw et al. 2002), which affects the production of cloud condensation nuclei. This pattern can be expressed as GCRs-cloud-climate. The flux of incoming GCRs is dependent on the solar activity and the strength of the geomagnetic field (Snowball & Muscheler 2006). High solar activity will decrease the incoming GCR flux, resulting in less cloud formation. Strong geomagnetic dipole field intensity will also decrease the incoming GCR flux (Snowball & Muscheler 2007). It has been assumed that the geomagnetic field strength contributes to the long-term changes in GCRs flux, whereas solar activity is primarily responsible for short-term variations of GCRs flux. Does the unusual variation of geomagnetic field around feature "f" influence the GCR flux significantly? Is the influence from geomagnetic field variation large or small compared with influence from solar activity? To quantify the impact of geomagnetic

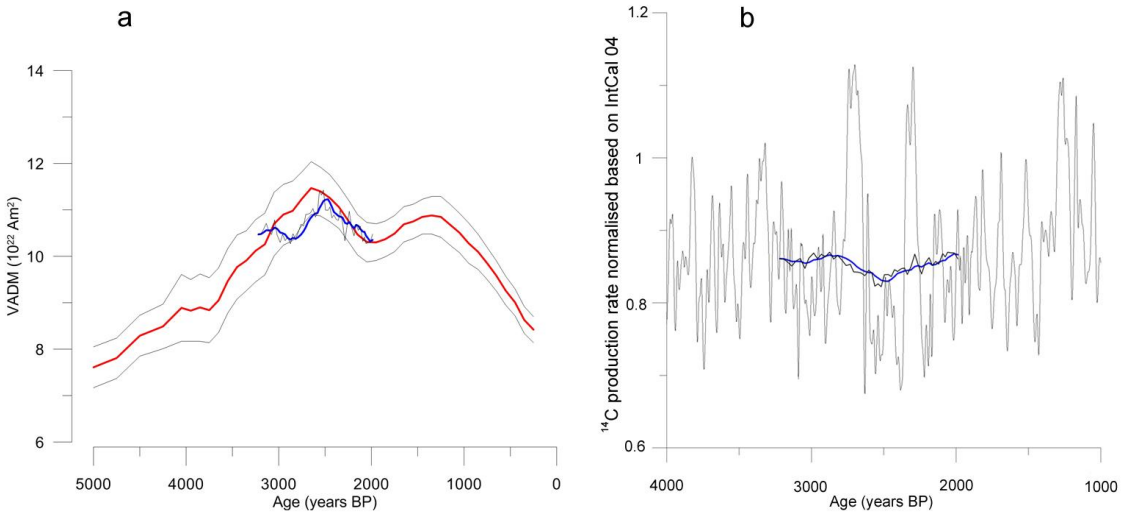

Fig. 24. *(a) Red line is the virtual axis dipole moment (VADM) reconstructed by Knudsen et al. (Knudsen et al. 2008). Blue line is the VADM calculated based on paleogeomagnetic intensity data from Gyltigesjön. (b) Comparison of overall ^{14}C production rate from IntCal04 (data provided by Raimund Muscheler) with ^{14}C production rate calculated based on paleogeomagnetic intensity data from Gyltigesjön.*

field variations on cosmogenic radionuclides reaching the atmosphere, the ^{14}C production variation caused by changes of geomagnetic intensity was calculated (Muscheler et al. 2005; Knudsen et al. 2008).

The result shows that that variation of geomagnetic field intensity around feature "f" does not affect ^{14}C production significantly (Fig. 24). High ^{14}C production rates in 2300 and 2700 yrs BP can be attributed to decreases of solar magnetic activity (which is assumed to reflect irradiance changes for the purpose of this study). Thus, if the GCRs-cloud -climate module is true, there will not be significant climate change caused by magnetic field changes during this period.

6 Conclusion

- Magnetic grains from sediment samples of Lake Gyltigesjön consist mainly of non-interacting SD magnetite grains, which are the preferred material for palaeomagnetic reconstructions. The relative palaeointensity reconstruction is reliable for the study period. In addition the reconstruction of inclination, declination and RPI from this study is similar to result in FENNOSTACK and FENNORPIS.
- The largest variation in climate proxies occurs at 2850 cal. yrs BP, which is most likely related to a short and intense period of human activity. This event is very local. It is unlikely that this signal is linked to the cooling event around 2.8 kyr BP. Subtle, human induced disturbances of the landscape probably took place at 2580 and 2320 cal. yrs BP. It is not likely these changes are produced by climate changes.
- There is no significant correlation between climate variations and RPI changes, based on proxies from this study and other studies in Southern Sweden. It is possible that the detected human impact on the environment has masked the true relationship between climate and geomagnetic intensity. More climate proxies and geomagnetic field reconstructions for areas less

influenced by human activity are needed.

- The influence of geomagnetic field intensity on radionuclide formation is limited for the study period. Thus, the GCRs-cloud-climate module cannot be used to explain any climate variations for the study period. Variation in solar activity is generally responsible for the centennial scale changes of radionuclide production during the 1st Millennium BC.
- Although the link between geomagnetic field changes and climate change is speculative, the age of declination feature 'f' and the relative palaeointensity peak associated with it make them useful isochrons for the correlation and relative dating of archives.

7 Possible improvement

Although difficult to interpret, it is believed that high resolution grey-scale measurement can provide important paleoclimate information. To measure grey scale information more precisely, a standard Kodak grey-scale can be put aside the sediment core when taking photos. With this standard grey-scale, calibration can be made to make grey scale values from different pictures comparable. Besides, plastic paper or even transparent glass sheet could be placed on top of the sediments to enhance the visibility of sediment by reducing reflection by water. To better interpret grey scale as a climate indicator, other parameters such as biogenic silica or authigenic $CaCO_3$ can be measured. Thin section can also be done to provide abundant information to help.

8 Acknowledgements

I would like to thank I. Snowball for giving me such a great opportunity to learn so much more about our planet. Thank you for instruction in both the paleomagnetic laboratory and the field. R. Muscheler is thanked for instructing me how to process my data and interpret. It was apleasant experience to work with A. Johansson on varve counting and photo recording of sediments. A. Johansson is also thanked for providing me the ^{14}C dating results. Å. Wallin is thanked for helping me with the preparation of pollen slides. I would like to thank A. Broström, Mats Rundgren, Karl Ljung and Lovisa Zillén for discussing results. I want to thank my parents L. Shuping and N. Jingsheng for supporting me during the two years in Sweden. My girlfriend, L. Tiantian, is thanked for encouraging me during tough times.

9 References

Anderson, R. Y. (1996), *Seasonal sedimentation: a framework for reconstructing climatic and environmental change*, 1-16 pp., Geological Society Special Publication, London.

Bard, E., and Delaygue, G. 2007: Comment on "Are there connections between the Earth's magnetic field and climate?" by V. Courtillot, Y. Gallet, J.-L. Le Mouël, F. Fluteau, A. Genevey EPSL 253, 328, 2007, *Earth and Planetary Science Letters*, *265*, 302-307.

Berglund, B. E. 2003: Human impact and climate changes—synchronous events and a causal link?, *Quaternary International*, *105*, 7-12.

Berglund, M. 1995: Late Weichselian shore displacement in Halland, southwestern Sweden: relative sea-level changes and their glacio-isostatic implications, *BOREAS*, *24*, 324-344.

Björck, S. 1987: The answer to the Ancylus enigma?-presentation of a working

thesis, *GFF*, 171-176.

Björkman, L. 2001: The role of human distrubance in Late Holocene vegetation changes on Kullaberg, southern Sweden, *Vegetation History and Archaeobotany*, *10*, 201-210.

Broström, A., Sugita, S., and Gaillard, M.-J. 2004: Pollen productivity estimates for the reconstruction of past vegetation cover in the cultural landscape of southern Sweden, *The Holocene*, *14*, 368-381.

Carslaw, K. S., Harrison, R. G., and Kirkby, J. 2002: Cosmic Rays, Clouds, and Climate, *Science*, *298*.

Courtillot, V., Gallet, Y., Mouël, J.-L. L., Fluteau, F., and Genevey, A. 2007: Are there connections between the Earth's magnetic field and climate?, *Earth and Planetary Science Letters*, *253*, 328-339.

Day, R., Fuller, M., and Schmidt, V. A. 1977: Hysteresis properties of titanomagnetites: Grain-size and compositional dependence, *Physics of the Earth and Planetary Interiors*, *13*, 260-267.

Dean, W., Anderson, R., Bradbury, J. P., and Anderson, D. 2002: A 1500-year record of climatic and environmental change in Elk Lake, Minnesota I: Varve thickness and gray-scale density, *Journal of Paleolimnology*, *27*, 287-299.

Digerfeldt, G. 1988: Reconstruction and regional correlation of Holocene lake-level fluctuations in Lake Bysjön, South Sweden, *Boreas*, *17*, 165-182.

Dunlop, D. J. 2002: Ratios such as Mrs/Ms and Hcr/Hc indicate domain state of magnetic mineral, which further indicate magnetic mineral grain size. , *Journal of Geophysical Research*, *107*.

Egli, R., Chen, A. P., Winklhofer, M., Kodama, K. P., and Horng, C.-S. 2010: Detection of noninteracting single domain particles using first-order reversal curve diagrams, *Geochemistry Geophysics Geosystems*, *11*, 22.

Gallet, Y., Genevey, A., and Fluteau, F. 2005: Does Earth's magnetic field secular variation control centennial climate change?, *Earth and Planetary Science Letters*, *236*, 339-347.

Geel, B. V., J.Buurman, and Waterbolk, H. T. 1996: Archaeological and palaeoecological indications of an abrupt climate chang inThe Netherlands, and evidence for climatological teleconnections around 2650 BP, *Journal of Quaternary Science*, *11*, 451-460.

Geel, B. V., Heusser, C. J., Renssen, H., and Schuurmans, C. J. E. 2000: Climatic change in Chile at around 2700 BP and global evidence for solar forcing: a hypothesis, *The Holocene*, *10*, 659-664.

Grimm, E. 1987: CONNIS: a FORTRAN 77 program for stratigraphical constrained cluster analysis by the method of incremental sum of squares, *Computers and Geosciences*, *13*, 13-37.

Grimm, E. 1991: Tilia 1.12, Tilia-Graph 1.18., *Springfield, Illinois: Illinois State Museum, Research and Colection Center*.

Gurhén, M., Bigler, C., and Renberg, I. 2007: Liming placed in a long-term perspective: a paleolimnological study of 12 lakes in the Swedish liming program, *J Paleolimnol*, *37*, 247-258.

Gurhén, M., Bindler, R., Korsman, T., Rosen, P., Wallin, J.-E., and Renberg, I. 2003: Paleolimnologiska undersökningar av kalkade referenssjöar Del 4., *Institutionen för ekologi och geovetenskap Umeå universitet*.

Haltia-Hovi, E., Nowaczyk, N., and Saarinen, T.

2011: Environmental influence on relative palaeointensity estimates from Holocene varved lake sediments in Finland, *Physics of the Earth and Planetary Interiors*, *185*, 20-28.

Heiri, G., Lotter, A. F., and Lemcke, G. 2001: Loss on ignition as a method for estimating organic and carbonate content in sediments: reproducibility and comparability of results, *Journal of paleolimnology*, *25*, 101-110.

Hughen, K. A., Overpeck, J. T., Peterson, L. C., and Trumbore, S. 1996: Rapid climate changes in the tropical Atlantic region during the last deglaciation, *Nature*, *380*, 51-54.

Jönsson, P., and Bärring, L. 1994: Zonal index variation, 1899 - 1992: Links to air temperature in southern Scandinavia, *Geografiska Annaler*, *76*, 209-219.

de. Jong, R. 2007: Stormy records from peat bogs in south-wsst Sweden - implications for regional climatic variability and vegetation changes during the past 6500 years, *Lundqua Thesis 58*.

Knudsen, M. F., and Riisager, P. 2009: Is there a link between Earth's magnetic field and low-latitude precipitation?, *Geology*, *37*, 71-74.

Knudsen, M. F., Riisager, P., Donadini, F., Snowball, I., Muscheler, R., Korhonen, K., and Pesonen, L. J. 2008: Variations in the geomagnetic dipole moment during the Holocene and the past 50 kyr, *Earth and Planetary Science Letters*, *272*, 319-329.

Lagerlund, E., and Houmark-Nielsen, M. 1993: Timing and pattern of the last deglaciation in the Kattegat region, southwest Scandinavia, *Boreas*, 337-347.

Muscheler, R., Beer, J., Kubik, P. W., and Synal, H.-A. 2005: Geomagnetic field intensity during the last 60,000 years based on ^{10}Be and ^{36}Cl from the Summit ice cores and ^{14}C, *Quaternary Science Reviews*, *24*, 1849-1860.

Nilsson, A. 2011: Assessing Holocene and late Pleistocene geomagnetic dipole field variability, *LUNDQUA Thesis*, *64*.

Parry, L. G. 1982: Magnetization of immobilized particle dispersions with two distinct particle sizes, *Physics of the Earth and Planetary Interiors*, *28*, 230-241.

Peck, J. A., Green, R. R., Shanahan, T., King, J. W., Overpeck, J. T., and Scholz, C. A. 2004: A magnetic mineral record of Late Quaternary tropical climate variability from Lake Bosumtwi, Ghana, *Palaeogeography, Palaeoclimatology, Palaeoecology*, *215*, 37-57.

Petterson, G. 1996: Varved sediments in Sweden: a brief review, *Palaeoclimatology and Palaeoceanography from Laminated Sediments.Geological Society Special Publication*, 73-77.

Renberg, I. 1982: Varved lake sediments - geochronological records of the Holocene, *GFF*, *104*, 275–279.

Roberts, A. P., Pike, C. R., and Verosub, K. L. 2000: Firstorder reversal curve diagrams: A new tool for characterizing the magnetic properties of natural samples, *Journal of Geophysical Research*, *105*, 461-475.

Snowball, I., and Sandgren, P. 2004: Geomagnetic field intensity changes in Sweden between 9000 and 450 cal BP: extending the record of barchaeomagnetic jerksQ by means of lake sediments and the pseudo-Thellier technique, *Earth and Planetary Science Letters*, *227*, 361-376.

Snowball, I., and Muscheler, R. 2006: Palaeomagnetic intensity data: an Achilles heel of solar activity reconstructions, *The Holocene*, *17*,

851-859.

Snowball, I., and Muscheler, R. 2007: Palaeomagnetic intensity data: an Achilles heel of solar activity reconstructions, *The Holocene*, *17*, 851-859.

Snowball, I., Sandgren, P., and Petterson, G. 1999: The mineral magnetic properties of an annually laminated Holocene lakesediment sequence in northern Sweden, *The Holocene*, *9*, 353-362.

Snowball, I., Zillén, L., and Gaillard, M.-J. 2002: Rapid early-Holocene environmental changes in northern Sweden based on studies of two varved lake-sediment sequences, *The Holocene*, *12*, 7-16.

Snowball, I., Zillén, L., Ojala, A., Saarinen, T., and Sandgren, P. 2007: FENNOSTACK and FENNORPIS: Varve dated Holocene palaeomagnetic secular variation and relative palaeointensity stacks for Fennoscandia, *Earth and Planetary Science Letters*, *255*, 106-116.

Snowball, I., Muscheler, R., Zille´n, L., Sandgren, P., Stanton, T., and Ljung, K. 2010: Radiocarbon wiggle matching of Swedish lake varves reveals asynchronous climate changes around the 8.2 kyr cold event, *BOREAS*, *29*, 720-733.

Stanton, T. 2011: High temporal resolution reconstructions of Holocene palaeomagnetic directions and intensity: an assessment of geochronology, feature reliability and enviromental bias, *LUNDQUA Thesis*, *63*.

Stanton, T., Snowball, I., Zillen, L., and Wastegård, S. 2010: Validating a Swedish varve chronology using radiocarbon, paleomagnetic secular variation, lead pollution history and statistical correlation, *Quaternary Geochronology*, *5*, 611-624.

Sugita, S. 2007: Theory of quantitative reconstruction of vegetation I: pollen from large sites REVEALS regional vegetation composition, *The Holocene*, *17*, 229-241.

Thompson, R., and Oldfield, F. (1986), *Environmental magnetism*.

Winklhofer, M., and Zimanyi, G. T. 2006: Extracting the intrinsic swichting field distribution in perpendicular media: A comparative analysis, *Journal of Applied Physics*, *99*.

Wohlfarth, B., Holmquist, B., Cato, I., and Linderson, H. 1997: The climatic significance of clastic varves in the Ångermana¨lven Estuary, northern Sweden, AD 1860 to 1950, *The Holocene*, *8*, 521-534.

Zillén, L., Snowball, I., Sandgren, P., and Stanton, T. 2003: Occurrence of varved lake sediment sequences in Värmland, west central Sweden: lake characteristics, varve chronology and AMS radiocarbon dating, *BOREAS*, *32*.

10 Appendix: Data used in this thesis and its contributor

Sediment-coring in Gyltigesjön	I. Snowball, A. Johansson, E. Ahlstrand, B. Lougheed, J. Striberger
Geomagnetic field reconstruction from Gyltigesjön (Declination, inclination and RPI)	E. Ahlstrand
Volume susceptibility (κ), Mass susceptibility (χ), Saturation isothermal remanent magnetization (SIRM)	E. Ahlstrand
Saturation magnetization (M_s), Saturation remanence (M_{rs}), coercive force ($(B_0)_C$) and coercivity of remanence ($(B_0)_{CR}$)	W. Ning, I. Snowball
Varve counting	W. Ning, A. Johansson
First order reversal curve (FORC) diagram	W. Ning, I. Snowball
Loss on ignition (LOI), Total carbon (TC), C/N, varve thickness, grey scale	W. Ning, Å. Wallin
Pollen analysis	W. Ning, A. Broström, Å. Wallin
^{14}C Wiggle-match dating	A. Johansson

Tidigare skrifter i serien "Examensarbeten i Geologi vid Lunds Universitet":

240. Bjärnborg, Karolina, 2009: The copper sulphide mineralisation of the Zinkgruvan deposit, Bergslagen, Sweden. (45 hskp)
241. Stenberg, Li, 2009: Historiska kartor som hjälp vid jordartsgeologisk kartering – en pilotstudie från Vångs by i Blekinge. (15 hskp)
242. Nilsson, Mimmi, 2009: Robust U-Pb baddeleyite ages of mafic dykes and intrusions in southern West Greenland: constraints on the coherency of crustal blocks of the North Atlantic Craton. (30 hskp)
243. Hult, Elin, 2009: Oligocene to middle Miocene sediments from ODP leg 159, site 959 offshore Ivory Coast, equatorial West Africa. (15 hskp)
244. Olsson, Håkan, 2009: Climate archives and the Late Ordovician Boda Event. (15 hskp)
245. Wollein Waldetoft, Kristofer, 2009: Sveko-fennisk granit från olika metamorfa miljöer. (15 hskp)
246. Månsby, Urban, 2009: Late Cretaceous coprolites from the Kristianstad Basin, southern Sweden. (15 hskp)
247. MacGimpsey, I., 2009: Petroleum Geology of the Barents Sea. (15 hskp)
248. Jäkel, O., 2009: Comparison between two sediment X-ray Fluorescence records of the Late Holocene from Disko Bugt, West Greenland; Paleoclimatic and methodological implications. (45 hskp)
249. Andersen, Christine, 2009: The mineral composition of the Burkland Cu-sulphide deposit at Zinkgruvan, Sweden – a supplemen-tary study. (15 hskp)
250. Riebe, My, 2009: Spinel group minerals in carbonaceous and ordinary chondrites. (15 hskp)
251. Nilsson, Filip, 2009: Föroreningsspridning och geologi vid Filborna i Helsingborg. (30 hskp)
252. Peetz, Romina, 2009: A geochemical characterization of the lower part of the Miocene shield-building lavas on Gran Canaria. (45 hskp)
253. Maria Åkesson, 2010: Mass movements as contamination carriers in surface water systems – Swedish experiences and risks.
254. Elin Löfroth, 2010: Elin Löfroth, 2010: A Greeland ice core perspective on the dating of the Late Bronze Age Santorini eruption. (45 hskp)
255. Óluva Ellingsgaard, 2009: Formation Evaluation of Interlava Volcaniclastic Rocks from the Faroe Islands and the Faroe-Shetland Basin. (45 hskp)
256. Arvidsson, Kristina, 2010: Geophysical and hydrogeological survey in a part of the Nhandugue River valley, Gorongosa National Park, Mozambique. (45 hskp)
257. Gren, Johan, 2010: Osteo-histology of Mesozoic marine tetrapods – implications for longevity, growth strategies and growth rates. (15 hskp)
258. Syversen, Fredrikke, 2010: Late Jurassic deposits in the Troll field. (15 hskp)
259. Andersson, Pontus, 2010: Hydrogeological investigation for the PEGASUS project, southern Skåne, Sweden. (30 hskp)
260. Noor, Amir, 2010: Upper Ordovician through lowermost Silurian stratigraphy and facies of the Borenshult-1 core, Östergötland, Sweden. (30 hskp)
261. Lewerentz, Alexander, 2010: On the occurrence of baddeleyite in zircon in silica-saturated rocks. (15 hskp)
262. Eriksson, Magnus 2010: The Ordovician Orthoceratite Limestone and the Blommiga Bladet hardground complex at Horns Udde, Öland. (15 hskp)
263. Lindskog, Anders, 2010: From red to grey and back again: A detailed study of the lower Kundan (Middle Ordovician) 'Täljsten' interval and its enclosing strata in Västergötland, Sweden. (15 hskp)
264. Rääf, Rebecka, 2010: Changes in beyrichiid ostracode faunas during the Late Silurian Lau Event on Gotland, Sweden. (30 hskp)
265. Petersson, Andreas, 2010: Zircon U-Pb, Hf and O isotope constraints on the growth versus recycling of continental crust in the Grenville orogen, Ohio, USA. (45 hskp)
266. Stenberg, Li, 2010: Geophysical and hydrogeological survey in a part of the Nhandugue River valley, Gorongosa National Park, Mozambique – Area 1 and 2. (45 hskp)
267. Andreasen, Christine, 2010: Controls of seafloor depth on hydrothermal vent temperatures - prediction, observation & 2D finite element modeling. (45 hskp)

268. März, Nadine, 2010: When did the Kalahari craton form? Constraints from baddeleyite U-Pb geochronology and geo-chemistry of mafic intrusions in the Kaapvaal and Zimbabwe cratons. (45 hskp)
269. Dyck, Brendan, 2010: Metamorphic rocks in a section across a Svecnorwegian eclogite-bearing deformation zone in Halland: characteristics and regional context. (15 hskp)
270. McGimpsey, Ian, 2010: Petrology and lithogeochemistry of the host rocks to the Nautanen Cu-Au deposit, Gällivare area, northern Sweden. (45 hskp)
271. Ulmius, Jan, 2010: Microspherules from the lowermost Ordovician in Scania, Sweden – affinity and taphonomy. (15 hskp)
272. Andersson, Josefin, Hybertsen, Frida, 2010: Geologi i Helsingborgs kommun – en geoturistkarta med beskrivning. (15 hskp)
273. Barth, Kilian, 2011: Late Weichselian glacial and geomorphological reconstruction of South-Western Scania, Sweden. (45 hskp)
274. Mashramah, Yaser, 2011: Maturity of kerogen, petroleum generation and the application of fossils and organic matter for paleotemperature measurements. (45 hskp)
275. Vang, Ina, 2011: Amphibolites, structures and metamorphism on Flekkerøy, south Norway. (45 hskp)
276. Lindvall, Hanna, 2011: A multi-proxy study of a peat sequence on Nightingale Island, South Atlantic. (45 hskp)
277. Bjerg, Benjamin, 2011: Metodik för att förhindra metanemissioner från avfallsdeponier, tillämpad vid Albäcksdeponin, Trelleborg. (30 hskp)
278. Pettersson, Hanna, 2011: El Hicha – en studie av saltstäppssediment. (15 hskp)
279. Dyck, Brendan, 2011: A key fold structure within a Sveconorwegian eclogite-bearing deformation zone in Halland, south-western Sweden: geometry and tectonic implications. (45 hskp)
280. Hansson, Anton, 2011: Torvstratigrafisk studie av en trädstamshorisont i Viss mosse, centrala Skåne kring 4 000 - 3 000 cal BP med avseende på klimat- och vattenståndsförändringar. (15 hskp)
281. Åkesson, Christine, 2011: Vegetationsutveck-lingen i nordvästra Europa under Eem och Weichsel, samt en fallstudie av en submorän, organisk avlagring i Bellinga stenbrott, Skåne. (15 hskp)
282. Silviera, Eduardo M., 2011: First precise U-Pb ages of mafic dykes from the São Francisco Craton. (45 hskp)
283. Holm, Johanna, 2011: Geofysisk utvärdering av grundvattenskydd mellan väg 11 och Vombs vattenverk. (15 hskp)
284. Löfgren, Anneli, 2011: Undersökning av geofysiska metoders användbarhet vid kontroll av den omättade zonen i en infiltrationsdamm vid Vombverket. (15 hp)
285. Grenholm, Mikael, 2011: Petrology of Birimian granitoids in southern Ghana - petrography and petrogenesis. (15 hp)
286. Thorbergsson, Gunnlaugur, 2011: A sedimentological study on the formation of a hummocky moraine at Törnåkra in Småland, southern Sweden. (45 hp)
287. Lindskog, Anders, 2011: A Russian record of a Middle Ordovician meteorite shower: Extraterrestrial chromite in Volkhovian-Kundan (lower Darriwilian) strata at Lynna River, St. Petersburg region. (45 hp)
288. Gren, Johan, 2011: Dental histology of Cretaceous mosasaurs (Reptilia, Squamata): incremental growth lines in dentine and implications for tooth replacement. (45 hp)
289. Cederberg, Julia, 2011: U-Pb baddelyit dateringar av basiska gångar längs Romeleåsen i Skåne och deras påverkan av plastisk deformation i Protoginzonen. (15 hp)
290. Ning, Wenxing, 2011: Testing the hypothesis of a link between Earth's magnetic field and climate change: a case study from southern Sweden focusing on the 1st millennium BC. (45 hp)

LUNDS UNIVERSITET

Geologiska institutionen
Lunds universitet
Sölvegatan 12, 223 62 Lund